Multimedia Tools and Applications (2020) 79:32415–32448
https://doi.org/10.1007/s11042-020-09664-1

Modified water wave optimization algorithm for underwater multilevel thresholding image segmentation

Zheping Yan [1] • Jinzhong Zhang [1] • Jialing Tang [1]

Received: 27 November 2019 / Revised: 15 July 2020 / Accepted: 18 August 2020 /
Published online: 27 August 2020

Abstract

Multilevel thresholding is a simple and important method for image segmentation in various applications that has drawn widespread attention in recent years. However, the computational complexity increases correspondingly when the threshold levels increase. To overcome this drawback, a modified water wave optimization (MWWO) algorithm with the elite opposition-based learning strategy and the ranking-based mutation operator for underwater image segmentation is proposed in this paper. The elite opposition-based learning strategy increases the diversity of the population and prevents the search from stagnating to improve the calculation accuracy. The ranking-based mutation operator increases the selection probability. MWWO can effectively balance exploration and exploitation to obtain the optimal solution in the search space. To objectively evaluate the overall performance of the proposed algorithm, MWWO is compared with six state-of-the-art meta-heuristic algorithms by maximizing the fitness value of Kapur's entropy method to obtain the optimal threshold through experiments on ten test images. The fitness value, the best threshold values, the execution time, the peak signal to noise ratio (PSNR), the structure similarity index (SSIM), and the Wilcoxon's rank-sum test are used as important metrics to evaluate the segmentation effect of underwater images. The experimental results show that MWWO has a better segmentation effect and stronger robustness compared with other algorithms and an effective and feasible method for solving underwater multilevel thresholding image segmentation.

Keywords Multilevel thresholding · Image segmentation · Water wave optimization · Elite opposition-based learning strategy · Ranking-based mutation operator · Kapur's entropy

✉ Jinzhong Zhang
zhangjinzhongz@126.com

[1] College of Automation, Harbin Engineering University, Harbin 150001, China

1 Introduction

Unmanned underwater vehicles (UUVs) with vision systems not only have the ability to acquire optical images and video information, but they are also able to perform image and video information processing, feature extraction and classification recognition. The mission of a UUV vision system is to quickly and accurately obtain information about underwater targets, then process the obtained information in real time, feed back the processing results to a computer network, and finally guide the UUV to perform the correct operation [17, 19, 23, 24, 30]. The three-dimensional model of a UUV equipped with a vision system is given in Fig. 1. Image segmentation is a crucial and basic process that divides a given image into several distinct regions and extracts the target object of interest from the complex scene. Image segmentation can retain the important structural feature information of an image while greatly reducing the amount of data to be processed in advanced processing stages such as image analysis and recognition. It is the basis for subsequent image understanding such as subsequent feature extraction and target recognition. Therefore, the success of image analysis depends on the reliability of the segmentation, and accurately segmenting images is often a challenging problem. Image segmentation methods can be divided into the following important categories: thresholding-based methods, region-based methods, edge-based methods, clustering-based methods and graph-based methods [13, 14, 32, 45, 46]. Compared with other methods, the thresholding-based method has certain advantages, such as simple operations, high computational efficiency, small storage space, strong robustness and fast processing speeds. Therefore, the thresholding-based method has attracted the attention of scholars and is used to solve the image segmentation problem. The thresholding-based method is divided into bi-level thresholding and multilevel thresholding according to the number of thresholds [9, 11]. The bi-level thresholding divides a given image into foreground and background, but it has certain limitations in solving complex images. When a given image contains a large amount of information and multiple objects, multilevel thresholding has a better segmentation effect and more stable performance.

Meta-heuristic algorithms are used to solve multilevel thresholding image segmentation, such as the bat algorithm (BA) [51], the flower pollination algorithm (FPA) [50], the moth swarm algorithm (MSA) [37], the particle swarm algorithm (PSO) [29], and the whale optimization algorithm (WOA) [36]. Zhou et al. proposed the MSA-

Fig. 1 Three-dimensional model equipped with a vision system

based Kapur's entropy to solve the image segmentation problem and verified the effectiveness and feasibility of the proposed algorithm [54]. Aziz et al. present the whale optimization algorithm and moth-flame optimization algorithm to obtain the optimal thresholds in image segmentation, and the proposed methods were found to be superior to other algorithms [16]. Quadfel et al. used the social spider algorithm and flower pollination algorithm as effective methods to solve image segmentation, and the results showed that the methods can balance the exploration and exploitation [38]. Díaz-Cortés et al. applied the dragonfly algorithm to solve multi-level thresholding for breast thermogram analysis, which was proved to be able to support reliable clinical decision making [15]. Sambandam et al. demonstrated the self-adaptive dragonfly algorithm using Kapur's entropy for image segmentation, and the results indicated that the proposed algorithm obtained the global best solution [41]. Sun et al. proposed a multi-level image threshold algorithm based a novel hybrid algorithm combining the gravitational search algorithm with the genetic algorithm and found that the proposed algorithm has a better segmentation effect [44]. Shen et al. developed a modified flower pollination algorithm to solve multilevel thresholding image segmentation, and the proposed algorithm was found to achieve high calculation accuracy and a fast convergence speed [43]. Gao et al. adopted an improved artificial bee colony algorithm to solve multi-level thresholding image segmentation, and the effectiveness of the proposed algorithm was verified [21]. Pare et al. proposed a firefly algorithm based on the Lévy flight strategy for image segmentation, and the results showed that the proposed algorithm enhanced the search performance and gained the optimal threshold values [40]. Pare et al. combined the cuckoo search algorithm with the minimum cross entropy for color image thresholding, and the results showed that the algorithm selected the optimal threshold values [39]. Satapathy et al. tried to combine the bat algorithm with the chaotic strategy and used the proposed algorithm for image thresholding [42]. Akay et al. conducted research based on using the particle swarm optimization algorithm and the artificial bee colony algorithm for image segmentation, and the results indicated that the algorithms are effective and feasible [7]. Bao et al. proposed the Harris Hawks optimization algorithm to solve the color image multilevel thresholding, and the experimental results revealed that the proposed algorithm is better than other algorithms [10]. Jia et al. a designed modified moth-flame algorithm to verify the overall performance in multi-level thresholding [26]. Bohat et al. applied the TH heuristic for color image segmentation, and the results showed that the proposed algorithm is superior to other algorithms [12]. Emberton et al. proposed a novel method to solve the underwater image and video dehazing problem, and the results showed that the method obtained the optimal effect [18]. Lu et al. proposed a neutrosophic C-means clustering with local information and a noise distance-based kernel metric, which was used to solve the image segmentation [35]. Galdran et al. proposed a red channel method to recover the colors with short wavelengths [20]. Hao et al. proposed an efficient nonlocal variational method to solve the image restoration problem, and the results evaluated its effectiveness and robustness [25]. Vasamsetti et al. present a wavelet based on the variational enhancement technique to cope with underwater imagery, and the results showed that the proposed method obtained the best result [47]. Li et al. proposed the MapReduce-based fast fuzzy c-means algorithm to deal with large-scale underwater image segmentation and the results showed that its segmentation effect is better than those of other methods [31]. Abualigah et al. combined the improved krill herd algorithm and a hybrid function to obtain promising and precise results in this domain, the results proved the proposed algorithm achieved almost all the best results for all datasets in comparision with the other comparative algorithms [6]. Abualigah reviewed the multiverse optimizer algorithm's main characteristics and procedures and recommended potential future research directions [1]. Abualigah et al. designed the hybrid particle swarm optimization algorithm with genetic operators to solve the text clustering problem, and the results showed that the proposed algorithm improved the clustering performance and obtained accurate clusters [3]. Abualigah et al. combined objective functions and the hybrid krill herd algorithm to solve the text document clustering problem, and the results showed that the proposed algorithm obtained the best results for all evaluation measures and datasets [5]. Abualigah et al. presented a new feature selection method based on the particle swarm optimization algorithm to improve the document clustering, and the results showed that the proposed method was effective and feasible [4]. Abualigah et al. created a novel hybrid antlion optimization algorithm for multi-objective task scheduling problems in cloud computing environments [2]. Liu et al. proposed a novel multichannel internet of things to dynamically share the spectrum with 5G communications, and the results indicated that the proposed method can improve the 5G throughput significantly [34]. Liu et al. proposed a cluster-based cognitive industrial internet of things to solve node transmissions via nonorthogonal multiple access [33].

Water wave optimization (WWO) is based on the shallow water theory, which mainly simulates propagation, refraction and breaking to obtain the global optimal solution [52]. The basic WWO has the disadvantages of premature convergence, low calculation accuracy and a slow convergence speed. To improve the overall optimization performance of the WWO, the elite opposition-based learning strategy [53] and the ranking-based mutation operator [22, 27] are added to WWO, and modified water wave optimization (MWWO) is proposed in this paper. MWWO based on Kapur's entropy method is applied to solve the underwater multilevel thresholding image segmentation problem. MWWO can effectively balance exploration and exploitation to obtain better segmentation accuracy. To verify the robustness and feasibility of the proposed algorithm, MWWO is compared with the BA [51], the FPA [50], the MSA [37], PSO [29], and the WWO [52], which lays a foundation for future research on underwater image.

The remainder of this article is divided into following sections. Section 2 introduces multilevel thresholding. Section 3 reviews basic WWO. Section 4 presents MWWO. In Section 5, the proposed MWWO-based multilevel threshold method is described in detail. The experimental results and analysis are provided in Section 6. Finally, conclusions and future research are drawn in Section 7.

2 Multilevel thresholding

The bi-level thresholding method and multilevel thresholding method occupy important positions in image segmentation. The bi-level thresholding method involves one threshold value and an image is divided into the foreground and background. That is to say, the bi-level thresholding method is effective and feasible for simple images. However, the method cannot be applied to complex images that contain multiple objects. Therefore, the multilevel thresholding method is used to segment complex images. The purpose of the optimization problem is to obtain the best values in the restricted space. Multilevel thresholding is transformed into an optimization problem that analyzes and finds the best threshold vectors by maximizing the objective function.

Kapur's entropy is an important and unsupervised technique, and it has been used extensively to solve the image segmentation problem by obtaining the optimal threshold values. The entropy of a given segmented image indicates the compactness and separateness between different classes. Assuming that $[t_1, t_2, \ldots, t_n]$ are the optimal threshold values based Kapur's entropy [28], an image is split into various classes. The formula is as follows:

$$p_i = \frac{h_i}{\sum_{i=0}^{L-1} h(i)} \tag{1}$$

where h_i is the number of pixels with gray level i, N is the total number of pixels, and L is the number of levels in a given image.

$$f(t_1, t_2, \ldots, t_n) = H_0 + H_1 + H_2 + \ldots + H_n \tag{2}$$

where

$$H_0 = -\sum_{i=0}^{t_1-1} \frac{p_i}{\omega_0} \ln \frac{p_i}{\omega_0}, \omega_0 = \sum_{i=0}^{t_1-1} p_i \tag{3}$$

$$H_1 = -\sum_{i=t_1}^{t_2-1} \frac{p_i}{\omega_1} \ln \frac{p_i}{\omega_1}, \omega_1 = \sum_{i=t_1}^{t_2-1} p_i \tag{4}$$

$$H_2 = -\sum_{i=t_2}^{t_3-1} \frac{p_i}{\omega_2} \ln \frac{p_i}{\omega_2}, \omega_2 = \sum_{i=t_2}^{t_3-1} p_i \tag{5}$$

$$H_n = -\sum_{i=t_n}^{L-1} \frac{p_i}{\omega_n} \ln \frac{p_i}{\omega_n}, \omega_n = \sum_{i=t_n}^{L-1} p_i \tag{6}$$

H_0, H_1, …, H_n are the Kapur's entropies of the distinct classes, and ω_0, ω_1, …, ω_n are the probabilities of each class.

3 WWO

WWO mimics propagation, refraction and breaking operations to solve the optimization problem and obtain the optimal solution. In WWO, each wave with wave height

h and wavelength λ represents a solution to a problem, and its fitness value is inversely proportional to the vertical distance to the seabed's depth. The closer the water wave is to the sea level, the higher the fitness value, the better the corresponding solution, the larger the wave height and the smaller the wavelength. The optimal solution performs local search in a small range, and the inferior solution performs global search in a large range. The illustration of the WWO model is given in Fig. 2, and the corresponding relationship between the practical problem and the shallow water wave model is shown in Table 1.

3.1 Propagation

The accumulation of the wave energy is accomplished by the water wave continuously propagating, and the motion process is considered to the transition process from deep water to shallow water. In WWO, each wave propagates to update the location, and the relationship between the original wave x and the new wave x' is as follows:

$$x'(d) = x(d) + rand(-1,1) \cdot \lambda L(d) \tag{7}$$

where $rand(-1, 1)$ is a uniformly distributed random number and $L(d)$ is the length of the dimension of the search space. The new location is outside the feasible range, it is reset to a random location within the valid range. If $f(x') > f(x)$, wave x' replaces wave$x$, and the wave height is $h_{\max}$. Conversely, wave x is unchanged and one is subtracted from the wave height to record the energy loss. The wavelength is updated as follows:

$$\lambda = \lambda \cdot \alpha^{-(f(x)-f_{\min}+\varepsilon)/(f_{\max}-f_{\min}+\varepsilon)} \tag{8}$$

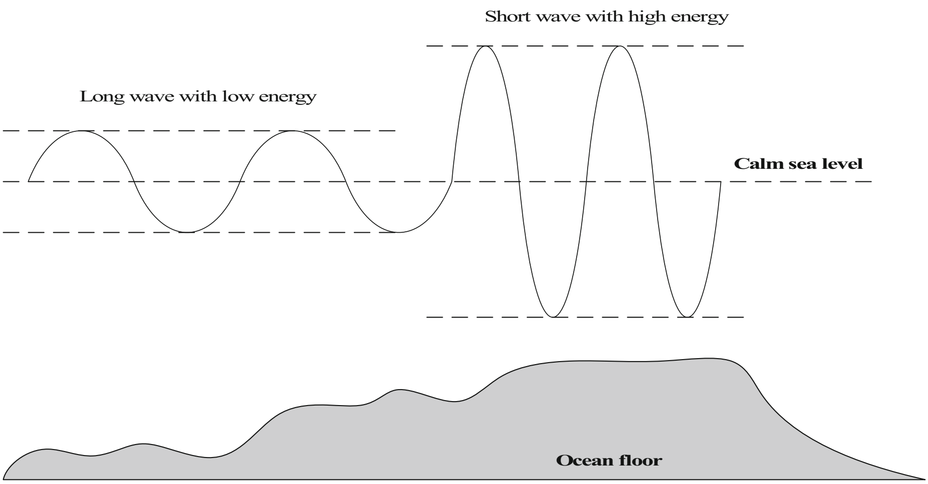

Fig. 2 Different wave shapes in deep and shallow water

Table 1 Correspondence between problem space and population space

Practical problem	Shallow water wave model
Search space	Seabed
Each solution	A water wave
Fitness value of each solution	It is inversely proportional to the vertical distance to seabed

where $f_{\max}$ and $f_{\min}$ are the maximum and minimum fitness values, respectively; $\alpha$is the wavelength reduction coefficient; and ε is a minimal positive number to avoid the divisor from being zero.

3.2 Refraction

The fitness value of wave x has not been improved after multiple propagation operations. With the continuous loss of energy, the wave height is attenuated to zero, and the wave x performs a refraction to avoid search stagnation. The location is updated as follows:

$$x^{'}(d) = N\left(\frac{(x^{*}(d) + x(d))}{2}, \frac{|x^{*}(d) - x(d)|}{2}\right) \tag{9}$$

where x^* is the optimal wave with the highest fitness value, and $N(\mu, \sigma)$ is a Gaussian random number with a mean of μ and a variance of σ. The wave height of new wave $x^{'}$ is reset t o$h_{\max}$, and wave x learns from the optimal wave x^* to enhance the global search ability and convergence speed. The wavelength is updated as follows:

$$\lambda^{'} = \lambda \frac{f(x)}{f(x^{'})} \tag{10}$$

3.3 Breaking

The increasing energy of a wave will make the wave crest increasingly steeper, and finally the wave will break into a series of solitary waves. The optimal wave performs the breaking operation and the specific operation randomly selects k dimensions (k is a random number from 1 to $k_{\max}$) to generate a solitary wave. The location is updated as follows:

$$x^{'}(d) = x(d) + N(0, 1) \cdot \beta L(d) \tag{11}$$

where β is the breaking coefficient. The updated k solitary waves have their fitness values evaluated. If the fitness value of a solitary wave is better than that of the original wave x^*, x^* is replaced. Otherwise, x^* is retained.

The basic WWO is shown in Algorithm 1.

Algorithm 1 WWO

1: Randomly initialize population p of n waves (solutions), wavelength λ, wave height $h_{\max}$, reduction coefficient α, breaking coefficient β, breaking directions $k_{\max}$.
2: Calculate fitness value of each wave and obtain optimal wave x^*
3: **While** stop criterion is not satisfied **do**
4: **For each wave** $x \in P$ **do**
5: Propagate wave x to a new wave x' using Eq. (7).
6: **If** $f(x') > f(x)$ **then**
7: **If** $f(x') > f(x^*)$, **then** wave x' perform breaking using Eq. (11), update optimal wave x^* with wave x'.
8: Replaces original wave x with a new wave x'
9: **Else**, decrease $x.h$ by one to indicate energy loss. **If** $x \cdot h = 0$, **then** wave x perform refraction using Eq. (9) and (10).
10: Update wavelengths λ using Eq. (8).
11: **End while**
12: **Return** optimal wave x^*.

4 MWWO

To overcome the shortcomings of falling into a local optimal solution and premature convergence, the elite opposition-based learning strategy and the ranking-based mutation operator are introduced into WWO to improve the calculation accuracy. MWWO can effectively obtain the global optimal solution.

4.1 Elite opposition-based learning strategy

The elite opposition-based learning strategy [53] is an effective search mechanism that can increase the population diversity and enhance the global search ability. After comparing the fitness values of the feasible solution and the inverse solution of each wave, the superior individual is regarded as elite wave $x_e = (x_{e,\ 1}, x_{e,\ 2}, \ldots, x_{e,\ D})$, The wave x_i and elite inverse solution $x_i^{'}$ are $x_i = (x_{i,\ 1}, x_{i,\ 2}, \ldots, x_{i,\ D})$ and $x_i^{'} = \left(x_{i,1}^{'}, x_{i,2}^{'}, \ldots, x_{i,D}^{'}\right)$, respectively, and the formula is as follows:

$$x_{i,j}^{'} = k \cdot \left(da_j + db_j\right) - x_{e,j}, i = 1, 2, \ldots, n; j = 1, 2, \ldots, D \tag{12}$$

where n is the size of the population, D is the search space dimension, $k \in U(0, 1)$, and da_j and db_j are the dynamic boundaries of jth decision variable. The latter are calculated as follows:

$$da_j = \min\left(x_{i,j}\right), db_j = \max\left(x_{i,j}\right) \tag{13}$$

The dynamic boundary of the search space replaces the fixed boundary, which is beneficial to preserving the optimal solution. The inverse solution jumps out (da_j, db_j) and is regarded as a feasible solution.

$$x'_{i,j} = rand\left(da_j, db_j\right), if x'_{i,j} < da_j or x'_{i,j} > db_j \tag{14}$$

4.2 Ranking-based mutation operator

To choose the optimal individual, it is necessary to sort each wave according to the related fitness values. First, the population is sorted in ascending order (i.e., from best to worst) based on the fitness value of each wave. The ranking of an individual is assigned as follows:

$$R_i = N_p - i, i = 1, 2, \ldots, N_p \tag{15}$$

The optimal wave in the current population will obtain the highest ranking, and N_p is the size of the population. After sorting the fitness value of each wave, the selection probability P_i of the *ith* wave is given as follows:

$$p_i = \frac{R_i}{N_p}, i = 1, 2, \ldots, N_p \tag{16}$$

The ranking-based mutation operator "DE/rand/1" is shown in Algorithm 2. The probability that the individual with a higher ranking is selected as the base vector or terminal vector in the mutation operator become larger, and the aim is to propagate the useful information from the current population to the offspring. The starting vector is not selected according to the selection probability, and the two vectors in the difference vector are obtained from better vectors. The corresponding step-size of the difference vector may decrease rapidly and lead to premature convergence [22, 27].

Algorithm 2 Ranking-based mutation operator of "DE/rand/1"

```
Sort the population, and assign the ranking and selection probability P_i for each wave
Randomly select r1 ∈ {1, N_p}   {base vector index}
While rand > p_r1 or r1 == i
    Randomly select r1 ∈ {1, N_p}
End
Randomly select r2 ∈ {1, N_p}   {terminal vector index}
While rand > p_r2 or r2 == r1 or r2 == i
    Randomly select r2 ∈ {1, N_p}
End
Randomly select r3 ∈ {1, N_p}   {starting vector index}
While r3 == r2 or r3 == r1 or r3 == i
    Randomly select r3 ∈ {1, N_p}
End
```

The ranking-based mutation operator increases the probability that a good individual is selected, and this enhances the exploitation ability. The elite opposition-based learning strategy increases the diversity of the population and enhances the exploration ability to improve the calculation accuracy. MWWO is shown in Algorithm 3.

Algorithm 3 MWWO

```
Randomly initialize population p of n waves (solutions), wavelength λ, wave height h_max, reduction coefficient α, breaking coefficient β, breaking directions k_max.
Calculate fitness value of each wave and obtain optimal wave x*
While stop criterion is not satisfied do
For each wave x ∈ P do
 Sort the population, and assign the ranking and selection probability P_i for each wave
/*ranking-based mutation stage*/
Randomly select r1 ∈ {1, N_p} {base vector index}
While rand > p_r1 or r1 == i
    Randomly select r1 ∈ {1, N_p}
End
Randomly select r2 ∈ {1, N_p} {terminal vector index}
While rand > p_r2 or r2 == r1 or r2 == i
    Randomly select r2 ∈ {1, N_p}
End
Randomly select r3 ∈ {1, N_p} {starting vector index}
While r3 == r2 or r3 == r1 or r3 == i
    Randomly select r3 ∈ {1, N_p}
End        /*end of ranking-based mutation stage*/
Propagate wave x to a new wave x', elite opposition-based learning strategy is introduced into propagation operation using Eq. (7).
If f(x') > f(x) then
If f(x') > f(x*), then wave x' perform breaking, elite opposition-based learning strategy is introduced into breaking operation using Eq. (11), update optimal wave x* with wave x'.
Replaces original wave x with a new wave x'
Else, decrease x.h by one to indicate energy loss. If x·h = 0, then wave x perform refraction, elite opposition-based learning strategy is introduced into refraction operation using Eq. (9) and (10).
Update wavelengths λ using Eq. (8).
End while
Return optimal wave x*.
```

5 MWWO-based multilevel threshold method

Water waves represent search agents. Their positions represent the image segmentation thresholds, and the fitness values of the waves are determined according to the change of the position. We update the optimal wave by comparing the fitness value and the optimal position provides the optimal threshold for segmentation. The correspondence between the image segmentation and MWWO space is given in Table 2. MWWO based on image segmentation is shown in Algorithm 4. The flowchart of MWWO for multilevel thresholding is shown in Fig. 3.

Algorithm 4 MWWO-based on image segmentation for Kapur entropy

Randomly initialize population p of N waves (solutions), wavelength λ, wave height $h_{\max}$, reduction coefficient α, breaking coefficient β, breaking directions $k_{\max}$, the maximum number of iterations is T, and the dimension of the problem is D.

Calculate fitness value of each wave using Eq. (2) for the Kapur-based method and obtain optimal wave x^*

While stop criterion is not satisfied **do**

For each wave $x \in P$ **do**

Sort the population, and assign the ranking and selection probability P_i for each wave

/*ranking-based mutation stage*/

Randomly select $r_1 \in \{1, N_p\}$ {base vector index}

While $rand > p_{r_1}$ or $r_1 == i$

  Randomly select $r_1 \in \{1, N_p\}$

End

Randomly select $r_2 \in \{1, N_p\}$ {terminal vector index}

While $rand > p_{r_2}$ or $r_2 == r_1$ or $r_2 == i$

  Randomly select $r_2 \in \{1, N_p\}$

End

Randomly select $r_3 \in \{1, N_p\}$ {starting vector index}

While $r_3 == r_2$ or $r_3 == r_1$ or $r_3 == i$

  Randomly select $r_3 \in \{1, N_p\}$

End /*end of ranking-based mutation stage*/

Propagate wave x to a new wave x', elite opposition-based learning strategy is introduced into propagation operation using Eq. (7).

If $f(x') > f(x)$ **then**

If $f(x') > f(x^*)$, **then** wave x' perform breaking, elite opposition-based learning strategy is introduced into breaking operation based on Eq. (11), update optimal wave x^* with wave x'.

Replace original wave x with a new wave x'

Else, decrease $x.h$ by one to indicate energy loss. **If** $x \cdot h = 0$, **then** wave x perform refraction, elite opposition-based learning strategy is introduced into refraction operation based on Eq. (9) and (10).

Update wavelengths λ based on Eq. (8).

End while

Return optimal wave x^*, which represents the optimal threshold values of segmentation.

Table 2 Correspondence between image segmentation and MWWO

Image segmentation problem space	MWWO space
A collection contains all the optimization schemes $(x_1, x_2, \ldots, x_k)$ to solve the image segmentation problem	A water wave population P with $(n_1, n_2, \ldots, n_k)$ waves
An optimal optimization scheme for solving the image segmentation problem	An optimal water wave
The objective evaluation function of the image segmentation problem	The fitness function of the MWWO

5.1 Complexity analysis

In this section, the time and spatial complexity of the proposed algorithm are analyzed.

5.1.1 Time complexity

The time complexity of MWWO is briefly analyzed in this subsection. MWWO mainly contains five steps: initialization, ranking-based mutation, propagation, breaking and refraction. If the population size is N, the maximum number of iterations is T, and the dimension of the problem is D. The time complexity of MWWO is described as follows. Step 1 requires $O(1)$. Step 2 requires $O(N)$. Steps 3, 4 and 5 require $O(N \times D \times T)$. Steps 6, 7, 8 and 9 require $O(1)$. Steps 10, 11, 12 and 13 require $O(1)$. Steps 14, 15, 16 and 17 require $O(1)$. Steps 18, 19, 20, 21, 22, 23 and 24 require $O(N \times D \times T)$. By considering all of the above steps, the total time complexity of MWWO is $O(N \times D \times T)$.

5.1.2 Spatial complexity

The spatial complexity of an algorithm is regarded as the storage space consumed by the algorithm. The total space complexity of MWWO is $O(N \times D \times T)$. The optimization algorithms are used to solve the spatial complexity according to the number of agents. Therefore, the space complexity of MWWO is effective and feasible.

6 Experimental results and analysis

6.1 Experimental setup

The numerical experiment is set up on a computer with an Intel Core i7-8750H 2.2 GHz CPU, a GTX1060, and 8 GB memory running on Windows 10.

6.2 Test images

The underwater optical vision system consists of three important parts: the bottom optical vision image acquisition system, the middle image processing system and the high-level underwater target recognition system. The system's task is to perform pre-processing, feature extraction and classification recognition on signal frame or video sequence images. A UUV with a vision system shoots underwater images, then applies image processing techniques to

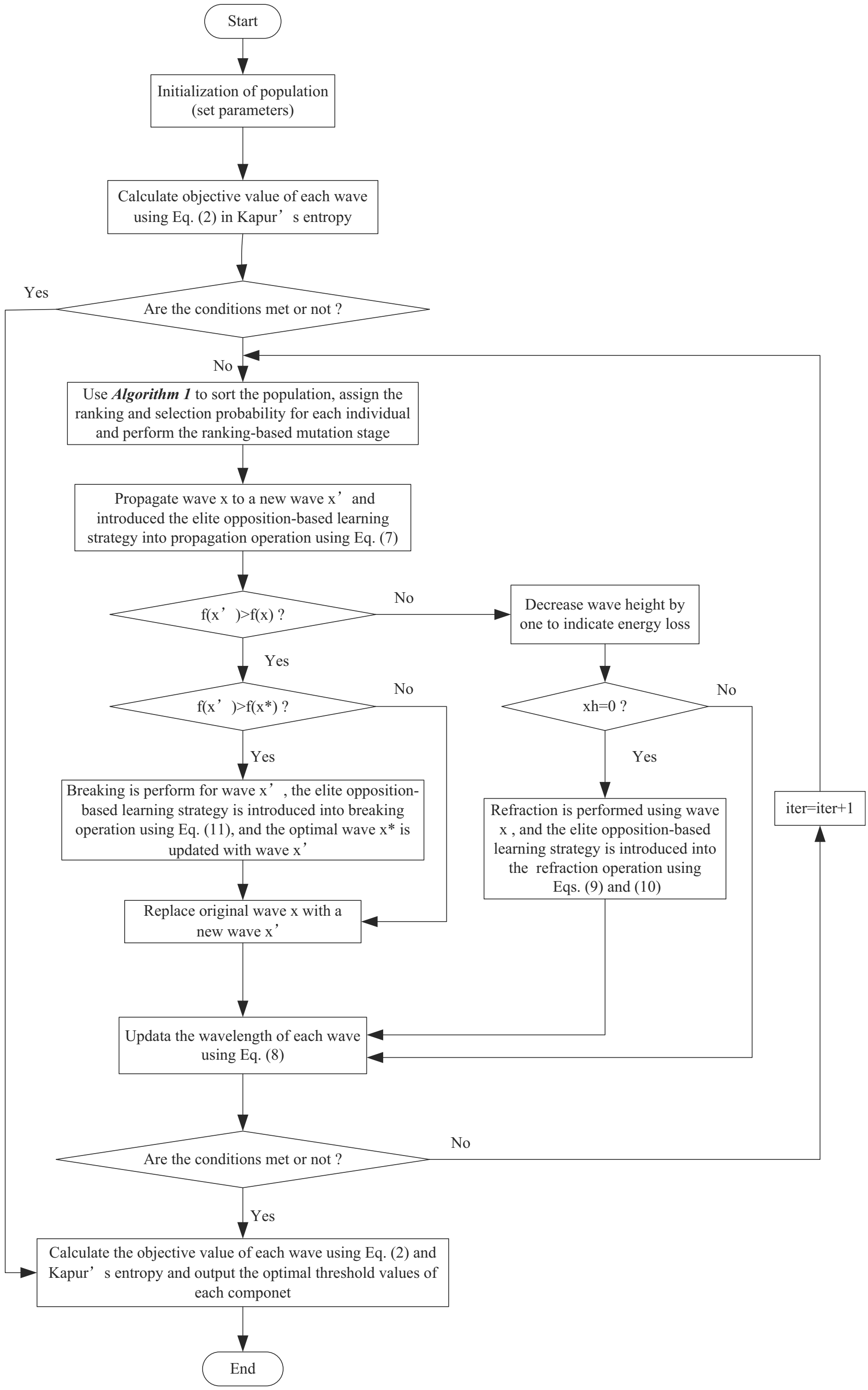

Fig. 3 Flowchart of MWWO for multilevel thresholding

obtain the target information and uses pattern recognition to complete the image understanding to achieve the purpose of environmental perception. The research goal of underwater image segmentation is to achieve fast, accurate, highly robust and adaptive segmentation. Image segmentation is a key step from image processing to image analysis, and is the key to achieving target feature extraction, recognition and tracking. Image segmentation divides a pre-processed underwater image to obtain an image that contains only the target and the background, making it more intuitive. The segmentation quality will directly affect the stability and reliability of the feature extraction, target recognition and tracking. Due to the diversity and complexity of underwater environments, the fluctuation of the water medium, the effects of light scattering, refraction and absorption, and the disturbance of suspended objects in the water, the underwater image has low contrast and distorted image features. Therefore, it is necessary to further study underwater image segmentation technology. The experiments address ten selected images to assess the effectiveness and feasibility of MWWO, and they are given in Fig. 4.

6.3 Parameter setting

The WWO based on the elite opposition-based learning strategy is named EWWO [52, 53], and the WWO based the ranking-based mutation operator is named RWWO [22, 27, 52]. To verify the superiority of the MWWO algorithm in underwater multilevel thresholding image segmentation, a total of eight algorithms (including the BA, the FPA, the MSA, PSO, the

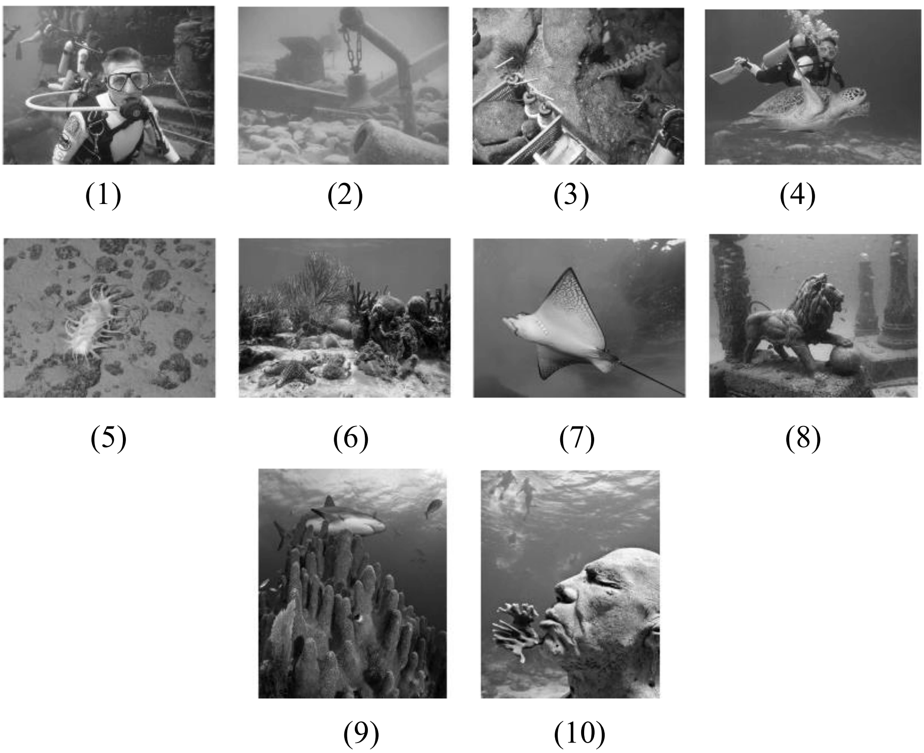

Fig. 4 Original test images

WWO, EWWO, RWWO and MWWO) are selected for the comparison experiments. The parameters of all algorithms are given in Table 3, and the control parameters are derived from the original paper and are representative empirical values.

6.4 Segmented image quality measurements

Five methods are applied to evaluate the overall performance of the segmented images, and the important metrics are utilized as follows.

(1) Fitness value. The information contained in the segmented image is closely related to the fitness value. The larger the fitness, the more information the segmented image contains.

Table 3 Parameters of all algorithms

Algorithms	Parameters	Values
BA [51]	Pulse frequency range f	[0,2]
	Echo loudness A	0.25
	Decreasing coefficient γ	0.5
FPA [50]	Switch probability ρ	0.8
MSA [37]	Random number θ	[−2,1]
	Random number ε_2	[0,1]
	Random number ε_3	[0,1]
	Random number r_1	[0,1]
	Random number r_2	[0,1]
PSO [29]	Constant inertia ω	0.3
	First acceleration coefficient c_1	1.4962
	Second acceleration coefficient c_2	1.4962
WWO [52]	Wavelength λ	0.5
	Wave height h_{max}	6
	Wavelength reduction coefficient α	1.0026
	Breaking coefficient β	[0.001,0.25]
	Maximum number k_{max} of breaking directions	min(12, D/2)
EWWO [52, 53]	Wavelength λ	0.5
	Wave height h_{max}	6
	Wavelength reduction coefficient α	1.0026
	Breaking coefficient β	[0.001,0.25]
	Maximum number k_{max} of breaking directions	min(12, D/2)
RWWO [22, 27, 52]	Wavelength λ	0.5
	Wave height h_{max}	6
	Wavelength reduction coefficient α	1.0026
	Breaking coefficient β	[0.001,0.25]
	Maximum number k_{max} of breaking directions	min(12, D/2)
	Scaling factor F	0.7
	Constant c_1	6.5025
	Constant c_2	58.5525
MWWO [22, 27, 52, 53]	Wavelength λ	0.5
	Wave height h_{max}	6
	Wavelength reduction coefficient α	1.0026
	Breaking coefficient β	[0.001,0.25]
	Maximum number k_{max} of breaking directions	min(12, D/2)
	Scaling factor F	0.7
	Constant c_1	6.5025
	Constant c_2	58.5525

(2) Execution time. Each algorithm runs 30 times independently to calculate the average execution time, and the time can objectively reflect the computational complexity. The less time that is taken, the faster the algorithm.

(3) Peak signal to noise ratio (PSNR). The PSNR is applied to evaluate the difference between the segmented image and the reference image according to the intensity value in the image, and the value represents the quality of the reconstructed image. The larger the PSNR value is, the lower the image distortion. However, it has some limitations. The visual acuity of human eyes is not absolute, which results in a PSNR value that may be inferior to a lower PSNR value. The PSNR is defined as follows [8]:

$$PSNR = 10\log_{10}\left(\frac{255^2}{MSE}\right) \tag{17}$$

where MSE is the mean squared error. It is defined as follows:

$$MSE = \frac{1}{MN}\sum_{i=1}^{M}\sum_{j=1}^{N}\left[I(i,j)-K(i,j)\right]^2 \tag{18}$$

where M and N represent the size of the original image and the segmented image respectively.

(4) Structure similarity index (SSIM). The SSIM is used to calculate the similarity between the original image and the segmented image in the range of [−1,1]. The larger the SSIM value, the better the segmented image. The SSIM is defined as follows [48]:

$$SSIM(\mathrm{x},\mathrm{y}) = \frac{\left(2\mu_x\mu_y + c_1\right)\left(2\sigma_{xy} + c_2\right)}{\left(\mu_x^2 + \mu_y^2 + c_1\right)\left(\sigma_x^2 + \sigma_y^2 + c_2\right)} \tag{19}$$

where μ_x and μ_y represent the mean intensity of the original image and the segmented image respectively. σ_x^2 and σ_y^2 represent the standard deviation of the original image and the segmented image respectively. σ_{xy} represent the covariance between the original image and the segmented image. c_1 and c_1 are both constants.

(5) Wilcoxon's rank-sum test. To further verify the superiority and feasibility of MWWO, the Wilcoxon's rank-sum test [49] was adopted. If the p value is less than 0.05, there is a significant difference between the algorithms, and the optimization performance is better than those of the other algorithms. If the p value is larger than 0.05, there is no significant difference between the algorithms.

6.5 Results and analysis

For a fair comparison, the population size of all algorithms is 30, the maximum number of iterations is 100, and the number of independent runs is 30. The numbers of thresholds are 2, 3, 4, 5 and 6, respectively. The MWWO based on Kapur's entropy method is used to solve the underwater multilevel thresholding image segmentation. The experimental results are compared with other algorithms that include the BA, the FPA, the MSA, PSO, the WWO. Meanwhile, to further verify that the elite opposition-based learning strategy and the ranking-based mutation operator can improve the calculation accuracy of the algorithm, ablation experiments are added to demonstrate this point. MWWO is compared with WWO based on the elite opposition-based learning strategy (EWWO) and WWO based on the ranking-based mutation operator (RWWO). The experimental results are given in Tables 4, 5, 6, 7, 8 and 9, and the comparison results of the segmented images are given in Figs. 5, 6, 7, 8, 9, 10, 11, 12, 13 and 14. All experimental data are based on the optimal fitness value, the set threshold value, the average execution time, the PSNR, the SSIM and the p value of Wilcoxon's rank-sum test.

Table 4 gives the optimal fitness values of each algorithm. The goal of image segmentation is to maximize the fitness value of Kapur's entropy method to obtain the optimal threshold. The numbers of thresholds are defined as 2, 3, 4, 5 and 6. It can be seen that as the number of thresholds increases, the fitness value will become larger, which means that different algorithms obtain higher segmentation accuracy when solving the image segmentation problem. To highlight the obviousness and superiority of MWWO, the ranking is based on the optimal fitness values. Ten underwater images are used to test the segmentation performance of all algorithms, and each image has five different threshold levels. That is, there are 50 fitness values for each algorithm. For MWWO, its number of best fitness values is 42. Compared with other algorithms, MWWO can avoid falling into the local optimum to obtain the global optimal solution. The fitness values of EWWO and RWWO are obviously better than that of the basic WWO, but the optimization performance of MWWO is the best. MWWO effectively balances the exploration and exploitation to obtain the optimal fitness values, which indicates that MWWO contains more information in the segmented images. Table 5 gives the best threshold values obtained by all the algorithms. The threshold value determines the quality and accuracy of image segmentation. Different algorithms are used to solve the underwater image segmentation problem, but MWWO can obtain relatively better threshold values so that the MWWO can achieve the best fitness values, which indicates that MWWO has strong robustness and better calculation accuracy.

Table 6 gives the average execution time of each algorithm. The larger the threshold level, the more time each algorithm consumes. MWWO can obtain the optimal fitness values and the best threshold values. Compared with the basic WWO, MWWO has the elite opposition-based learning strategy and the ranking-based mutation operator added, which improve the convergence accuracy of the basic WWO and enhances the image segmentation effect to a certain extent. However, MWWO consumes more time to complete the underwater multilevel thresholding image segmentation compared to WWO, EWWO and RWWO. The average execution time of MWWO is better than those of the other algorithms. The experimental results show that MWWO can effectively complete the underwater image segmentation task and obtain a higher segmentation accuracy.

Table 7 gives the PSNRs of each algorithm. The underwater image segmentation accuracy is close to the threshold levels, and the optimization algorithm can obtain higher segmentation accuracy under a higher threshold level. The PSNR not only assesses the difference between the segmented image and the original image, but it is also a criterion for image segmentation to assess the segmentation performance of each algorithm. The PSNRs of MWWO based on Kapur's entropy method are compared with these of the other algorithms based on Kapur's

Table 4 The optimal fitness of each algorithm

Images	K	Fitness values								
		BA	FPA	MSA	PSO	WWO	EWWO	RWWO	MWWO	Rank
Test 1	2	12.7085	12.8868	12.8347	12.9208	12.8177	12.8935	12.8598	12.9199	2
	3	15.8480	15.6663	15.7008	15.8257	15.8528	15.9079	15.7695	15.9202	1
	4	18.7319	18.6094	18.7294	18.5727	18.3434	18.8079	18.6190	18.8465	1
	5	21.0754	21.2313	21.3045	21.2645	21.3326	21.0075	21.4241	21.4442	1
	6	23.4016	23.7049	23.8085	23.6672	23.6850	23.7356	23.6908	23.9723	1
Test 2	2	10.4629	10.3831	10.3951	10.4259	10.4553	10.4618	10.4040	10.4645	1
	3	12.8546	12.7759	12.8350	12.8106	12.8219	12.8519	12.8741	12.8883	1
	4	14.9544	14.8416	14.6897	14.7958	14.6831	14.9114	14.9313	14.9713	1
	5	16.8160	16.7859	16.8103	16.8387	16.6747	17.1013	17.0344	16.9308	3
	6	18.7121	18.7256	18.8425	18.6415	18.8036	18.5910	18.4234	18.9002	1
Test 3	2	12.8969	12.8948	12.8957	12.9240	12.8638	12.8897	12.8416	12.9210	2
	3	15.9517	16.0350	15.8704	15.9036	15.6777	15.8926	16.0784	16.0947	1
	4	18.9358	18.8556	18.8669	18.6685	18.8558	18.6959	18.7127	18.9954	1
	5	21.6187	21.4811	21.4157	21.2278	21.2551	21.2138	21.6126	21.6209	1
	6	23.5809	23.7746	23.7763	23.7578	23.7284	24.0417	23.4979	23.7846	2
Test 4	2	12.1512	12.0303	12.0564	12.2072	12.2163	12.2073	12.1908	12.2821	1
	3	15.3002	15.3391	15.2195	15.3544	14.9766	14.9965	15.0902	15.5041	1
	4	17.9560	17.9314	17.9423	17.9433	18.0839	18.0296	18.0959	18.1017	1
	5	20.5251	20.1917	20.5303	20.5470	20.5344	20.5875	20.3928	20.5886	1
	6	23.1096	22.6675	22.6342	22.4341	22.4060	22.9306	23.1381	23.1596	1
Test 5	2	11.7380	11.6097	11.7898	11.7040	11.8527	11.7748	11.7113	11.8945	1
	3	14.8898	14.7014	14.5522	14.6917	14.6251	14.7169	14.4587	14.9206	1
	4	17.1686	17.1820	17.2142	16.9222	17.0299	17.4527	17.3498	17.5419	1
	5	19.6665	19.6335	19.6171	19.5398	19.6203	19.7036	19.5024	19.7533	1
	6	21.9956	21.8207	21.9703	21.9284	21.7126	22.0673	22.7118	22.1803	2
Test 6	2	12.6094	12.6542	12.5621	12.6496	12.5435	12.6452	12.6086	12.6744	1
	3	15.7020	15.7752	15.6045	15.7632	15.8056	15.6656	15.6484	15.8781	1
	4	18.2725	18.5491	18.5348	18.3686	18.4223	18.5649	18.5411	18.5958	1
	5	21.4280	21.0965	21.0246	21.4343	21.2878	20.9344	21.0198	21.5643	1
	6	23.9853	23.9794	23.6006	23.7282	23.9050	24.0596	24.0684	24.1915	1
Test 7	2	12.0660	12.0851	11.9959	12.4321	12.0004	12.0350	12.0454	12.2668	2

Table 4 (continued)

Images	K	Fitness values								
		BA	FPA	MSA	PSO	WWO	EWWO	RWWO	MWWO	Rank
	3	15.1121	15.0188	15.1441	14.9729	15.0684	15.2013	15.1861	15.2563	1
	4	17.7446	17.8559	17.7886	17.6041	17.9319	18.2090	17.7566	18.4281	1
	5	20.9236	20.3856	20.1737	20.9267	20.2188	20.6392	20.5848	21.1350	1
	6	22.9995	22.9567	23.0321	22.8631	22.7462	23.2135	23.2483	23.2733	1
Test 8	2	11.9405	11.8608	11.8428	11.9988	11.8690	12.0572	11.9756	12.0417	2
	3	14.9328	14.8146	14.8768	15.0608	15.0242	14.9433	15.0210	15.1669	1
	4	17.8527	17.7700	17.8844	17.6650	17.8128	17.8095	17.8447	17.9075	1
	5	20.2234	20.4435	20.1689	20.2899	20.5645	20.5651	20.5779	20.7022	1
	6	22.8716	22.7048	22.8690	22.7195	22.8246	22.9240	22.8318	22.9356	1
Test 9	2	12.8823	12.8814	12.8145	12.8158	12.8096	12.8644	12.9110	12.9128	1
	3	15.7875	15.9264	15.9306	15.8615	15.8879	15.9827	15.9430	15.9945	1
	4	18.8978	18.8430	18.9199	18.8583	18.8297	18.7409	18.8881	18.9825	1
	5	21.5743	21.3246	21.4997	21.5816	21.5051	21.7865	21.4666	21.5109	4
	6	23.8370	23.9340	24.0520	23.8814	23.9948	23.8884	24.0562	24.0642	1
Test 10	2	12.9401	12.9879	12.8814	12.9817	12.9590	12.9675	12.9492	13.0039	1
	3	16.1837	16.0476	16.1094	16.0689	16.1175	16.1865	16.1211	16.2493	1
	4	19.1408	19.1239	19.0466	19.1551	19.2587	19.2896	19.1831	19.2963	1
	5	21.5383	21.2045	21.6062	21.8497	21.5127	21.9013	21.8652	21.9764	1
	6	24.1146	24.1043	24.2730	24.5451	24.3571	24.4032	24.2402	24.7640	1

Table 5 The best threshold values of each algorithm

Images	K	BA	FPA	MSA	PSO	WWO	EWWO	RWWO	MWWO
Test 1	2	110,192	96,157	105,177	93,161	110,176	98,169	105,172	94,160
	3	75,168,215	48,126,192	59,128,199	59,95,166	81,116,162	86,156,216	92,173,201	78,158,192
	4	74,100,170, 215	63,99,169, 232	68,136,169, 220	91,146,170, 201	69,86,119, 166	80,120,165, 219	48,86,117, 183	78,112,169, 202
	5	73,116,139, 174,236	83,109,155, 189,208	64,103,170, 196,234	71,93,130, 156,225	60,97,118, 151,206	84,99,136, 179,228	64,96,136, 174,225	60,100,152, 190,230
	6	35,63,118, 133,178,231	41,95,157, 183,215,233	52,113,136, 163,198,213	40,82,147, 164,183,218	37,52,83, 126,155,193	45,82,132, 158,180,207	80,100,147, 170,191,223	53,75,91, 133,163,208
Test 2	2	126,170	139,174	124,161	131,173	125,170	131,170	134,174	130,171
	3	94,141,169	124,147,166	109,145,173	111,149,172	122,143,175	101,131,167	99,126,162	121,146,173
	4	109,133,147, 167	104,121,136, 172	89,100,138, 168	112,134,151, 183	99,125,135, 180	97,127,138, 163	93,120,135, 172	91,122,144, 178
	5	105,128,141, 167,190	91,101,133, 154,168	93,118,129, 151,188	84,86,144, 156,208	91,103,123, 161,177	100,117,127, 154,174	91,112,123, 146,171	94,130,146, 160,183
	6	96,123,143, 159,180,193	86,98,123, 150,170,188	106,121,136, 148,169,187	88,110,120, 144,164,183	98,120,132, 149,158,182	99,113,136, 166,174,191	97,120,158, 172,188,198	92,108,129, 140,162,174
Test 3	2	84,158	110,181	109,183	94,171	91,189	97,159	105,196	98,170
	3	84,137,216	71,125,173	88,126,165	53,134,201	46,94,145	69,108,199	69,135,198	82,135,186
	4	57,102,166, 201	85,122,154, 215	57,97,150, 219	76,142,161, 202	77,143,184, 212	60,82,158, 208	34,80,145, 204	75,114,157, 214
	5	36,81,130, 162,212	35,74,103, 169,210	37,61,104, 145,185	80,97,157, 194,219	64,83,107, 145,180	44,120,140, 191,222	74,115,157, 186,212	38,90,124, 174,217
	6	45,56,111, 139,161,197	43,76,134, 177,192,210	44,92,125, 170,203,213	26,57,92, 152,194,217	76,93,132, 156,187,234	55,89,114, 160,188,234	28,56,77, 125,196,217	60,89,140, 187,218,233
Test 4	2	130,179	121,211	134,175	126,183	110,195	115,196	120,170	108,175
	3	50,104,189	54,125,203	93,141,179	100,149,198	59,161,211	103,151,173	123,174,203	56,112,185
	4	76,110,150, 205	49,112,149, 223	44,87,141, 198	88,114,170, 208	50,85,128, 191	50,88,118, 193	54,99,142, 211	93,130,166, 210
	5	65,108,163, 201,232	65,83,107, 142,217	55,120,134, 177,224	42,115,154, 183,205	47,100,150, 203,235	56,99,145, 166,224	56,136,181, 201,227	70,105,159, 193,216
	6	62,94,138, 149,181,213	39,60,75, 129,177,214	43,102,138, 189,217,238	23,52,84, 134,144,175	42,85,133, 141,165,200	32,53,89, 121,148,195	56,73,103, 151,188,227	53,121,145, 168,201,218
Test 5	2	76,154	66,159	113,168	79,164	91,160	109,171	81,151	111,159
	3	104,156,209	69,117,166	92,166,216	77,111,166	58,108,150	104,165,198	96,177,211	108,155,206
	4	52,85,146, 189	38,102,152, 205	92,140,166, 202	66,86,130, 152	84,134,178, 204	72,99,149, 207	85,133,158, 201	54,115,153, 181
	5	51,78,121, 183,204	98,112,147, 181,206	65,111,141, 156,174	61,105,173, 203,215	37,87,113, 149,182	54,110,154, 164,215	52,118,172, 201,215	46,119,155, 171,201
	6	50,85,92, 125,157,202	59,90,132, 176,192,205	93,108,134, 166,192,211	63,88,122, 140,186,221	55,68,118, 137,156,172	38,55,88, 121,167,217	49,99,119, 155,183,214	52,84,121, 149,157,201
Test 6	2	118,186	84,152	128,178	86,155	42,137	86,150	96,157	73,150
	3	43,123,206	87,137,176	71,161,207	38,131,179	93,133,187	39,101,174	51,89,176	79,134,181
	4	70,84,126, 195	39,91,130, 155	64,104,153, 204	89,116,144, 206	37,93,134, 223	47,118,153, 190	47,102,157, 182	44,92,163, 214
	5	28,90,124, 178,205	35,82,117, 167,239	53,106,125, 144,200	45,79,120, 181,231	43,83,138, 199,223	54,124,142, 203,228	37,52,125, 150,189	44,95,131, 184,211
	6	31,98,123, 145,177,203	51,70,90, 122,154,198	20,65,96, 156,181,200	28,46,73, 129,188,222	42,70,107, 130,164,207	52,97,128, 163,192,237	35,70,94, 120,176,230	45,74,99, 127,154,188
Test 7	2	88,131	141,198	77,148	46,134	43,175	95,135	132,186	37,138
	3	76,129,181	44,117,175	44,105,129	38,156,219	51,156,190	86,129,193	86,135,211	50,82,144
	4	95,131,162, 190	24,54,142, 191	71,97,140, 185	32,53,92, 172	49,86,159, 182	40,106,165, 200	68,87,135, 183	46,86,154, 208
	5	39,64,111, 156,200	47,129,140, 166,215	44,119,150, 168,188	55,93,128, 181,204	29,55,127, 190,233	36,110,148, 185,221	41,58,135, 164,224	39,66,129, 163,204
	6	43,56,110, 130,163,225	20,47,63, 144,166,197	36,78,138, 152,194,233	39,117,136, 153,174,194	19,73,87, 132,186,215	25,51,110, 136,169,211	32,94,133, 145,172,213	48,82,148, 165,198,229
Test 8	2	91,200	87,130	63,126	98,209	86,139	101,203	115,177	114,203
	3	85,113,167	75,162,198	97,136,184	98,139,208	76,137,180	54,93,167	58,100,168	80,130,208
	4	78,145,173, 200	52,78,132, 172	75,145,175, 215	54,146,168, 213	68,124,175, 234	83,118,173, 201	56,78,135, 203	56,108,171, 229
	5	61,80,98, 146,209	75,117,135, 168,222	49,138,160, 180,205	47,76,156, 206,233	62,121,182, 202,233	89,129,172, 201,220	58,114,148, 204,229	68,103,151, 171,202
	6	51,101,121, 175,218,231	49,73,82, 140,166,202	37,76,96, 131,188,213	44,67,142, 178,197,228	52,73,96, 138,187,233	34,71,106, 133,170,206	69,84,107, 147,187,209	68,87,141, 172,197,232
Test 9	2	91,176	82,165	107,190	110,159	81,177	91,141	84,149	95,171

Table 5 (continued)

Images	K	Best threshold values							
		BA	FPA	MSA	PSO	WWO	EWWO	RWWO	MWWO
	3	37,129,168	77,153,230	75,135,167	108,146,189	78,162,227	74,111,174	64,102,149	97,148,190
	4	56,119,171, 222	29,69,119, 172	33,105,139, 192	48,114,139, 195	78,106,170, 232	51,123,145, 189	49,86,154, 233	49,108,164, 201
	5	37,68,122, 172,195	29,70,98, 191,224	41,65,127, 175,219	36,67,129, 154,229	31,63,90, 160,224	48,99,153, 183,223	25,46,98, 156,196	48,65,109, 146,185
	6	73,117,129, 168,189,226	47,61,79, 130,183,234	18,96,142, 170,204,230	25,84,155, 174,192,231	29,54,89, 162,212,228	74,107,127, 182,209,238	64,79,103, 160,193,233	70,125,146, 177,212,233
Test 10	2	80,143	85,174	84,140	66,158	69,177	75,182	78,187	71,154
	3	48,123,179	33,122,196	78,130,170	39,146,198	77,153,186	63,112,195	35,105,171	75,130,184
	4	41,108,143, 216	54,86,163, 200	77,126,172, 226	34,74,155, 216	45,85,158, 198	44,108,160, 213	75,124,158, 201	33,80,142, 190
	5	24,105,127, 179,221	62,91,140, 184,246	45,83,98, 145,180	30,106,143, 178,225	19,62,93, 161,186	63,103,148, 177,212	71,111,155, 181,210	35,86,116, 180,212
	6	65,91,119, 179,200,222	61,95,128, 143,165,194	42,90,128, 173,198,210	20,68,105, 129,163,203	27,59,98, 115,145,212	49,68,113, 146,196,236	44,87,111, 144,161,228	48,78,111, 141,170,208

Table 6 The average execution time of each algorithm

Images	K	Execution time (in second)							
		BA	FPA	MSA	PSO	WWO	EWWO	RWWO	MWWO
Test 1	2	2.8574	3.0751	5.9272	3.9123	2.2533	2.3883	2.4213	2.4971
	3	2.8088	3.0481	5.2032	4.7184	2.6301	2.6844	2.7061	2.8993
	4	3.1145	3.2714	5.4854	5.3488	3.2049	3.3517	3.4369	3.4658
	5	3.1103	3.3546	5.4506	5.8726	3.3790	3.8260	3.6406	4.0448
	6	3.6198	3.4154	5.3877	6.1127	3.7131	3.9746	3.9684	4.0197
Test 2	2	2.3749	2.8180	4.8679	3.6571	2.8877	2.9324	2.8904	2.9347
	3	2.5268	2.7638	5.1973	3.9300	2.5410	2.8288	2.7128	2.7274
	4	2.6855	2.9801	5.2891	4.2525	2.4124	2.8488	3.3883	3.4362
	5	3.1953	3.5255	5.7376	4.9667	3.2495	3.2969	3.3695	3.4351
	6	5.2643	5.6228	7.5633	6.9607	5.1520	5.8089	5.8531	5.8554
Test 3	2	2.7775	2.8299	5.5372	4.1831	2.1555	2.3549	2.4154	2.5153
	3	2.8914	3.1136	5.4950	5.1889	3.0900	3.2041	3.3441	3.4061
	4	3.1816	3.4255	5.3693	5.5945	3.0271	3.2978	3.1811	3.4961
	5	3.4067	3.4635	5.5421	5.6685	3.2969	3.3125	3.4715	3.6354
	6	3.5809	3.2997	5.0123	5.9550	3.4240	3.7342	3.6747	3.9645
Test 4	2	2.8240	2.9691	5.3616	4.3064	2.0741	2.0730	2.3028	2.8391
	3	2.9902	3.0969	5.3498	4.9519	3.6152	3.6425	3.6775	3.6934
	4	3.0347	3.1748	5.5380	5.4340	3.6021	3.8212	3.4912	3.4884
	5	3.1399	4.0046	5.3474	5.6001	3.5070	3.5456	3.8254	3.8405
	6	3.3971	3.2673	5.4806	5.7346	3.8160	3.9507	3.9783	4.0554
Test 5	2	2.7582	2.8129	5.0868	4.1224	2.3410	2.3566	2.3856	2.4114
	3	2.8300	2.9898	5.2533	4.4690	2.4563	2.7358	2.7173	2.7436
	4	3.0262	3.4599	7.4966	5.1224	3.0345	3.0804	3.5665	3.6935
	5	3.0425	3.1285	5.0364	5.2939	3.0375	3.0994	3.1148	3.1250
	6	3.2059	3.2338	5.3631	5.7045	3.6724	3.7432	3.6917	3.8053
Test 6	2	2.7305	2.9730	5.1655	4.3090	3.0674	3.1312	3.3101	3.7262
	3	3.0286	3.4338	5.3792	4.8892	3.5195	3.3754	3.4328	3.5645
	4	3.2537	3.7384	5.5040	5.5261	3.4620	3.5094	3.4646	3.5898
	5	3.5968	3.3882	5.3123	5.8092	3.2118	3.4642	3.4969	3.5112
	6	3.6907	3.3283	5.3616	5.9635	3.9429	3.9798	3.9358	4.0878
Test 7	2	2.7067	3.1583	5.1597	4.5004	3.1272	3.2194	3.3392	3.6237
	3	3.0591	3.2904	5.3275	4.8576	3.1878	3.2468	3.2623	3.8689
	4	3.4351	3.2674	5.0151	5.3279	3.2219	3.5055	3.5761	3.9353
	5	3.3643	3.5427	5.4200	5.6066	3.7070	3.7241	3.8181	3.8388
	6	3.2029	3.2264	5.3048	5.7828	3.9041	3.9095	3.8033	3.9312
Test 8	2	2.6352	3.3562	5.0774	4.1403	3.4979	3.6402	3.6372	3.6833
	3	2.9525	3.3508	5.0721	4.9442	3.0139	3.0788	3.1108	3.1909
	4	3.0930	3.1811	6.2394	5.3145	3.3487	3.2713	3.2864	3.2808
	5	3.2184	3.2691	5.3642	5.6269	3.1787	3.6077	3.4531	3.6611
	6	3.0864	3.3419	5.4421	5.8353	3.1478	3.2142	3.5784	3.6265
Test 9	2	3.0592	3.5658	5.2387	4.3335	3.3141	3.3991	3.4081	3.5668
	3	3.0982	3.2899	5.2751	5.0637	3.5558	3.6147	3.7002	3.7164
	4	3.3690	3.2775	5.4648	5.5484	3.2872	3.4813	3.6890	3.8021
	5	3.9472	3.4660	5.4735	5.9601	3.5052	3.6253	3.7918	3.9674
	6	3.7763	3.5734	5.4821	6.0854	3.7057	3.9593	3.8519	4.0356
Test 10	2	2.8009	2.8354	5.1954	4.2655	3.3753	3.3528	3.3662	3.5885
	3	2.9649	3.1212	5.7449	4.6910	3.2879	3.3066	3.3630	3.6091
	4	3.2856	3.4440	5.5375	5.4820	3.3582	3.6299	3.7632	3.9793
	5	3.4668	3.3279	5.5323	6.1515	3.4733	3.6764	3.5336	3.8555
	6	3.7380	3.3420	5.5348	6.1670	3.6284	3.6993	3.7995	3.8053

entropy method. By increasing the number of thresholds, the PSNRs increase significantly, which indicates that the optimization algorithm has better image segmentation quality. The

Table 7 The PSNR of each algorithm

Images	K	PSNR values								
		BA	FPA	MSA	PSO	WWO	EWWO	RWWO	MWWO	Rank
Test 1	2	50.3149	50.9708	50.5370	51.1401	50.3149	50.8669	50.5370	52.4339	1
	3	52.6689	51.3263	51.0819	51.3263	52.0265	51.6082	51.2000	52.9207	1
	4	52.7955	54.4345	53.6305	51.2625	53.4810	52.1217	57.8965	56.6290	2
	5	52.9207	51.8484	54.2633	53.1923	54.9853	51.7655	54.2633	54.9857	1
	6	53.6305	54.9857	56.8943	58.3667	56.1074	58.5981	52.1217	59.0699	1
Test 2	2	52.4739	51.7852	53.4796	52.5770	53.3205	52.5770	52.2749	53.3205	2
	3	54.6254	53.4796	57.6582	56.7725	53.7837	62.4563	64.2698	64.2698	1
	4	57.6582	59.9912	63.7078	56.4697	64.2698	65.6708	68.4281	69.7673	1
	5	59.3484	69.7673	68.4281	77.9737	69.7673	63.7078	69.7673	66.9800	6
	6	66.2208	66.9800	58.9172	59.9912	64.8263	64.2698	65.6708	69.1728	1
Test 3	2	51.3626	50.9567	50.9969	51.6255	51.7646	51.4906	51.1574	51.8599	1
	3	52.1172	53.0626	51.9091	52.5603	52.7965	53.2573	53.2573	54.6813	1
	4	54.8479	52.0621	54.8479	52.6350	52.5603	54.3678	60.9614	57.7166	2
	5	54.8479	54.2223	53.0626	52.3596	53.8230	57.7166	52.7965	59.4568	1
	6	54.8479	52.8810	55.6027	54.0838	52.6350	55.2062	63.6994	56.9717	2
Test 4	2	48.9074	48.9891	48.9891	48.9074	49.2003	49.1006	49.0074	49.2448	1
	3	61.6799	56.6994	60.7778	60.7778	59.8706	49.3768	48.9549	61.0387	2
	4	52.4056	61.1622	62.7711	50.3123	61.6799	61.6799	61.2551	60.3539	6
	5	56.6994	56.6994	59.8706	61.0387	58.7479	61.0387	61.0387	61.6799	1
	6	58.1856	64.1762	63.0237	81.6842	63.3007	68.6697	61.0387	82.4001	1
Test 5	2	53.5953	57.6844	53.5953	54.6524	56.3985	54.0793	58.0335	58.1149	1
	3	54.6524	61.7530	56.2376	59.3103	66.2381	54.6524	55.6473	70.7377	1
	4	53.4637	55.5133	56.2376	62.8685	57.6844	60.7662	57.4743	68.1569	1
	5	69.6474	55.3810	63.2574	64.8673	59.0509	68.1569	69.1393	72.4014	1
	6	57.8977	65.7678	56.0844	64.0342	67.6683	78.2683	70.7377	69.1393	3
Test 6	2	49.7230	53.0487	49.4743	52.9589	53.5816	52.9589	52.5529	53.6463	1
	3	56.6117	52.9156	53.7805	57.2570	52.6721	57.1204	55.7255	58.3388	1
	4	53.8526	57.1204	54.3817	52.8312	57.4022	56.1507	56.1507	58.3388	1
	5	56.7355	57.2570	55.5101	56.3752	53.5816	55.4038	57.4022	57.5452	1
	6	58.3388	55.7255	61.1145	58.8954	56.7355	55.6174	57.6933	56.3752	6
Test 7	2	53.0771	67.9299	54.6136	65.4452	66.2792	52.0802	48.8516	67.6805	2
	3	54.8401	66.0148	66.0148	66.7745	63.5499	53.2989	53.2989	67.9299	1
	4	52.0802	65.1241	56.0784	63.1005	64.3910	64.9910	56.9787	65.4452	1
	5	67.2215	65.1241	66.0148	61.8575	61.0730	67.1299	66.7745	67.2225	1
	6	66.5261	63.9634	67.9299	67.2225	62.6934	70.9752	68.9109	69.8162	2
Test 8	2	51.9080	52.1391	50.8508	51.5288	52.2001	51.3889	50.8508	52.5680	1
	3	52.2647	53.1692	51.5801	51.5288	53.0526	56.8014	56.0437	53.1692	3
	4	52.8433	55.6767	53.1692	51.3426	54.2009	52.4056	56.4199	56.4199	1
	5	55.4920	53.1692	57.8625	58.3517	55.3014	52.0204	56.0437	55.6767	4
	6	57.4144	57.8625	61.4334	59.1497	57.2025	62.6731	54.0330	60.6950	3
Test 9	2	50.5957	50.1411	50.0940	50.0284	49.9627	50.5957	50.6525	50.6868	1
	3	50.8366	51.4204	51.5705	50.0723	51.3502	51.6518	52.5771	52.9034	1
	4	53.5034	53.0186	51.5705	52.4703	51.3502	54.1724	54.4617	54.4617	1
	5	56.7049	58.6448	55.8752	56.9400	58.1496	54.6163	59.4837	59.4956	1
	6	51.7306	54.7796	62.2566	59.7837	58.6448	51.6518	52.5771	62.6949	1
Test 10	2	56.0172	55.4169	55.5371	56.5148	53.0406	56.6349	56.2692	57.0803	1
	3	60.3657	63.5308	56.2692	56.8627	56.3935	57.9972	63.0681	59.8338	4
	4	61.7650	59.3262	56.3935	63.3017	60.9501	61.1554	56.6349	63.5308	1
	5	65.5804	58.1297	60.9501	64.1890	66.9570	57.9972	57.0803	67.6660	1
	6	57.7497	58.2598	61.5524	66.6511	64.8594	60.1893	61.1554	68.4780	1

elite opposition-based learning strategy increases the diversity of the population and the ranking-based mutation operator improves the selection probability. Both of these improve

Table 8 The SSIM of each algorithm

Images	K	SSIM values								
		BA	FPA	MSA	PSO	WWO	EWWO	RWWO	MWWO	Rank
Test 1	2	0.3003	0.3409	0.3209	0.3656	0.3006	0.3495	0.3201	0.4228	1
	3	0.4506	0.3748	0.3519	0.3586	0.4165	0.3868	0.3654	0.4574	1
	4	0.4867	0.5661	0.4881	0.3513	0.4842	0.4443	0.6325	0.6090	2
	5	0.4684	0.4207	0.5593	0.4945	0.5770	0.4182	0.5556	0.5857	1
	6	0.5393	0.6009	0.5943	0.6428	0.6345	0.6806	0.4425	0.6986	1
Test 2	2	0.3885	0.3827	0.4447	0.4376	0.4373	0.4277	0.4200	0.4624	1
	3	0.4988	0.4247	0.6063	0.5754	0.4785	0.6670	0.6687	0.6845	1
	4	0.5611	0.6341	0.6745	0.5572	0.6806	0.6479	0.6903	0.7005	1
	5	0.6159	0.7260	0.6847	0.7436	0.7210	0.6571	0.6877	0.7455	1
	6	0.6588	0.6543	0.6079	0.6235	0.6326	0.6821	0.6555	0.6891	1
Test 3	2	0.3900	0.3611	0.3633	0.4048	0.3936	0.3919	0.3606	0.4142	1
	3	0.4698	0.5209	0.4491	0.5012	0.5131	0.4994	0.5292	0.5683	1
	4	0.6297	0.4974	0.6312	0.4891	0.4981	0.5967	0.7210	0.6631	2
	5	0.6459	0.6152	0.5698	0.5341	0.6094	0.6634	0.5509	0.7556	1
	6	0.6635	0.5752	0.6215	0.6227	0.5705	0.6892	0.7190	0.7277	1
Test 4	2	0.1115	0.1180	0.1201	0.1107	0.1405	0.1312	0.1181	0.1439	1
	3	0.7847	0.6893	0.7859	0.7884	0.7648	0.1584	0.1172	0.7964	1
	4	0.4693	0.7795	0.7507	0.2586	0.7415	0.7329	0.7859	0.7863	1
	5	0.6763	0.6324	0.7152	0.7531	0.7068	0.716	0.7530	0.7684	1
	6	0.6765	0.7669	0.7581	0.8017	0.7363	0.8182	0.7644	0.8549	1
Test 5	2	0.4938	0.6222	0.4928	0.5494	0.6060	0.5325	0.5825	0.6237	1
	3	0.5433	0.6085	0.5886	0.6289	0.6311	0.5451	0.5725	0.6837	1
	4	0.4268	0.4552	0.4785	0.5375	0.4879	0.6748	0.4832	0.6733	2
	5	0.6953	0.5709	0.6340	0.7171	0.6174	0.7049	0.6562	0.6413	5
	6	0.6048	0.6577	0.5558	0.6485	0.6508	0.7346	0.7230	0.7060	3
Test 6	2	0.2361	0.5701	0.2071	0.5674	0.5843	0.5654	0.5442	0.5863	1
	3	0.6684	0.5891	0.6039	0.6765	0.5759	0.6490	0.6505	0.6768	1
	4	0.6463	0.7293	0.6254	0.5431	0.7419	0.6648	0.6830	0.7696	1
	5	0.7378	0.6978	0.6384	0.7602	0.6127	0.6141	0.7365	0.7670	1
	6	0.7742	0.7484	0.8309	0.7920	0.7348	0.7382	0.7861	0.7598	5
Test 7	2	0.5570	0.7985	0.6610	0.8153	0.8192	0.4886	0.0866	0.8269	1
	3	0.6368	0.8302	0.7873	0.8533	0.8333	0.5560	0.5911	0.8539	1
	4	0.4352	0.8535	0.6841	0.7746	0.8341	0.8483	0.7267	0.8542	1
	5	0.8394	0.7393	0.7569	0.7734	0.8075	0.8129	0.8652	0.8413	2
	6	0.8266	0.7862	0.8410	0.7332	0.7914	0.8819	0.8112	0.8442	2
Test 8	2	0.4427	0.3864	0.3717	0.4220	0.3906	0.4120	0.3625	0.4767	1
	3	0.4500	0.4578	0.3986	0.3922	0.4800	0.6025	0.5923	0.5150	3
	4	0.4282	0.5919	0.4445	0.3903	0.5526	0.4836	0.6047	0.6452	1
	5	0.5674	0.5013	0.5693	0.6459	0.5817	0.4236	0.5944	0.5769	4
	6	0.6656	0.6409	0.7266	0.6605	0.6656	0.7182	0.5495	0.7115	3
Test 9	2	0.3500	0.2977	0.2882	0.2797	0.2682	0.3417	0.3585	0.3595	1
	3	0.3729	0.4358	0.4444	0.2828	0.4254	0.4547	0.5134	0.5274	1
	4	0.5736	0.5603	0.4564	0.5079	0.4427	0.5884	0.6389	0.6303	2
	5	0.7203	0.7424	0.6838	0.7165	0.7283	0.6481	0.7266	0.7472	1
	6	0.4428	0.6564	0.7071	0.7351	0.7685	0.4499	0.5565	0.7860	1
Test 10	2	0.5657	0.5905	0.5417	0.6135	0.4780	0.6210	0.6107	0.6212	1
	3	0.6740	0.6748	0.6045	0.6449	0.6327	0.6539	0.6902	0.6913	1
	4	0.7091	0.7276	0.6328	0.7504	0.7435	0.7361	0.6401	0.7383	3
	5	0.7220	0.7168	0.7306	0.7432	0.7627	0.7183	0.6753	0.7504	2
	6	0.6950	0.6982	0.7518	0.7891	0.7519	0.7711	0.7412	0.8036	1

the calculation accuracy and robustness of the basic WWO so that MWWO can effectively improve the global search ability and local search ability to obtain the optimal solution. To

Table 9 The *p value* of Wilcoxon rank-sum

Images	K	Wilcoxon test						
		BA	FPA	MSA	PSO	WWO	EWWO	RWWO
Test 1	2	4.69E-02	1.96E-10	3.95E-01	2.93E-08	4.20E-10	6.70E-11	7.04E-07
	3	6.41E-01	3.37E-05	4.62E-10	4.28E-08	3.02E-11	4.23E-03	1.47E-07
	4	3.76E-04	8.07E-01	3.02E-11	7.96E-03	4.20E-10	4.80E-07	9.51E-06
	5	1.44E-02	1.26E-01	3.02E-11	5.32E-03	3.02E-11	5.61E-05	2.83E-08
	6	2.84E-04	1.37E-03	3.02E-11	2.70E-02	3.02E-11	1.49E-04	7.12E-09
Test 2	2	1.50E-02	2.24E-04	3.52E-07	3.75E-01	4.61E-10	6.06E-11	1.20E-08
	3	2.16E-01	4.73E-02	3.02E-11	3.94E-04	4.50E-11	5.32E-03	3.01E-07
	4	4.50E-02	8.07E-01	3.02E-11	3.78E-01	4.50E-11	7.96E-03	3.96E-08
	5	2.92E-05	1.17E-03	3.02E-11	2.63E-01	3.02E-11	1.58E-02	1.10E-08
	6	1.10E-04	1.24E-03	3.02E-11	6.62E-01	3.69E-11	6.84E-01	4.62E-10
Test 3	2	3.95E-01	6.12E-10	9.93E-02	4.56E-11	2.67E-09	6.72E-10	6.36E-05
	3	1.86E-01	1.29E-09	3.52E-07	2.85E-11	8.99E-11	1.91E-02	5.97E-09
	4	2.62E-03	1.30E-01	3.02E-11	3.79E-01	1.09E-10	3.37E-05	1.85E-08
	5	1.33E-09	7.98E-02	3.02E-11	6.73E-01	4.98E-11	8.35E-08	1.70E-08
	6	1.25E-04	3.32E-06	3.02E-11	1.82E-01	2.87E-10	8.66E-05	8.48E-09
Test 4	2	5.79E-01	1.69E-09	0.032651	3.85E-09	4.20E-10	8.15E-11	7.77E-09
	3	4.84E-02	8.20E-07	7.39E-11	5.88E-05	1.09E-10	5.86E-06	6.53E-08
	4	8.74E-06	3.55E-01	3.02E-11	7.48E-02	1.96E-10	1.61E-06	3.81E-07
	5	6.35E-05	2.15E-02	3.02E-11	3.79E-01	7.39E-11	1.00E-03	9.26E-09
	6	8.48E-09	2.02E-08	3.02E-11	2.32E-02	1.09E-10	8.20E-07	5.57E-10
Test 5	2	8.42E-01	3.83E-06	3.03E-03	2.35E-06	1.46E-10	7.39E-11	2.00E-06
	3	3.71E-02	2.23E-01	8.15E-11	3.14E-05	9.76E-10	1.25E-05	1.07E-07
	4	1.86E-01	3.39E-02	3.02E-11	9.51E-06	5.57E-10	4.64E-05	1.85E-08
	5	1.38E-06	1.68E-03	3.02E-11	4.38E-01	3.02E-11	1.58E-04	3.82E-09
	6	1.22E-02	9.83E-08	3.02E-11	9.88E-03	3.34E-11	2.62E-03	6.52E-09
Test 6	2	7.73E-01	7.73E-01	1.17E-04	2.93E-08	3.02E-11	2.39E-08	3.08E-08
	3	3.24E-02	2.05E-03	2.61E-10	9.15E-09	3.69E-11	1.25E-04	7.09E-08
	4	2.88E-03	9.82E-01	3.02E-11	1.85E-01	1.33E-10	2.13E-04	1.07E-07
	5	2.91E-11	2.68E-04	3.02E-11	4.12E-02	4.98E-11	1.34E-05	1.56E-08
	6	1.08E-06	1.73E-06	3.02E-11	1.73E-03	1.61E-10	3.09E-06	1.73E-06
Test 7	2	6.31E-01	1.29E-06	4.64E-03	9.76E-11	5.49E-11	9.26E-09	4.71E-04
	3	5.83E-03	1.68E-03	1.10E-08	3.37E-02	4.98E-11	1.52E-03	2.23E-09
	4	1.95E-03	8.19E-01	3.02E-11	1.11E-06	3.02E-11	1.77E-03	3.65E-08
	5	7.06E-05	9.05E-02	3.02E-11	3.40E-01	3.02E-11	3.16E-05	5.97E-09
	6	4.69E-06	8.48E-09	3.02E-11	9.05E-02	5.49E-11	1.30E-03	1.70E-08
Test 8	2	6.20E-01	1.11E-06	2.50E-03	6.34E-06	3.34E-11	1.31E-08	1.17E-05
	3	2.52E-02	3.83E-06	4.62E-10	1.97E-07	6.07E-11	5.56E-04	2.15E-06
	4	1.03E-06	6.20E-01	1.46E-10	7.96E-03	3.02E-11	4.04E-03	1.43E-08
	5	7.15E-06	6.91E-04	3.02E-11	6.63E-01	2.23E-09	4.21E-02	3.47E-10
	6	9.51E-06	9.26E-09	3.02E-11	2.68E-06	4.98E-11	8.24E-04	3.82E-09
Test 9	2	1.15E-02	2.38E-07	2.76E-03	3.71E-07	9.92E-11	1.01E-08	1.61E-06
	3	5.01E-01	5.26E-04	3.69E-11	2.95E-08	3.82E-10	2.62E-03	9.52E-04
	4	1.93E-03	2.84E-01	3.69E-11	1.85E-01	5.00E-09	3.57E-06	2.57E-07
	5	2.46E-06	3.83E-05	3.02E-11	1.82E-03	1.09E-10	1.63E-02	1.01E-08
	6	1.59E-05	5.96E-09	3.02E-11	2.98E-04	6.70E-11	4.43E-03	3.82E-10
Test 10	2	4.38E-02	6.53E-08	3.85E-03	2.93E-08	3.81E-07	9.26E-09	1.25E-05
	3	5.89E-01	2.84E-04	3.16E-10	1.75E-08	2.37E-10	3.27E-02	7.60E-07
	4	3.36E-04	7.07E-01	3.02E-11	6.62E-01	6.07E-11	9.52E-04	4.69E-08
	5	4.47E-02	5.86E-06	3.02E-11	1.41E-02	3.02E-11	1.49E-06	1.20E-08
	6	2.64E-01	1.24E-03	3.02E-11	5.95E-03	3.34E-11	3.98E-04	7.60E-07

reflect the superiority of MWWO, a ranking is carried out based on the sizes of the PSNRs. The higher the ranking is, the better the PSNRs. Each algorithm has 50 PSNRs, and 35 PSNRs

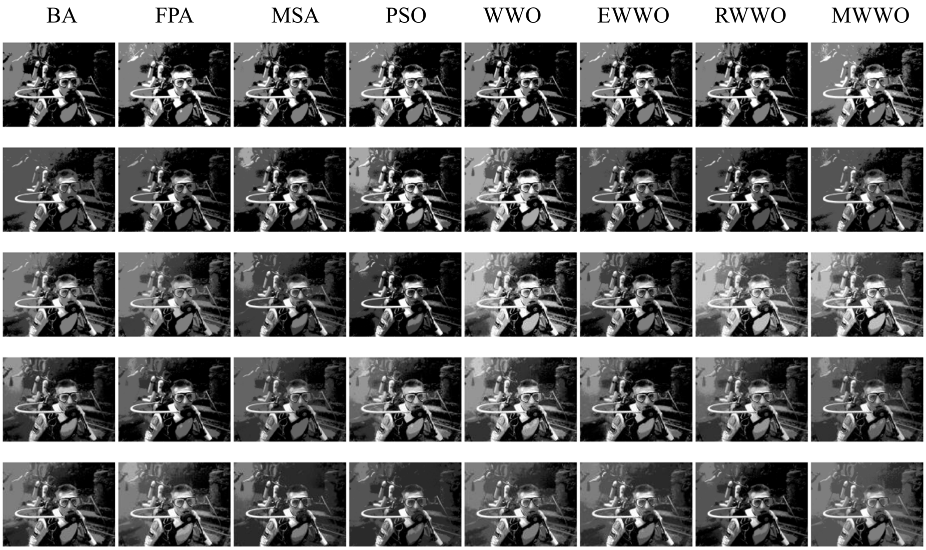

Fig. 5 Segmented images of Test 1

of MWWO are the best in all algorithms. The experimental results show that MWWO has stronger robustness and a better segmentation effect.

Table 8 gives the SSIMs of each algorithm. The SSIM is used to assess the visual similarity of the segmented image and the original image. The SSIMs increase as the threshold level increases, which indicates that the segmented images obtained by the optimization algorithms have less distortion and are closer to the original images. MWWO can avoid premature convergence and jump out of the local optimum to obtain better fitness values. To verify the image segmentation effect of MWWO, the ranking is based on the size of the SSIMs. The higher the ranking is, the more imgae segmentation

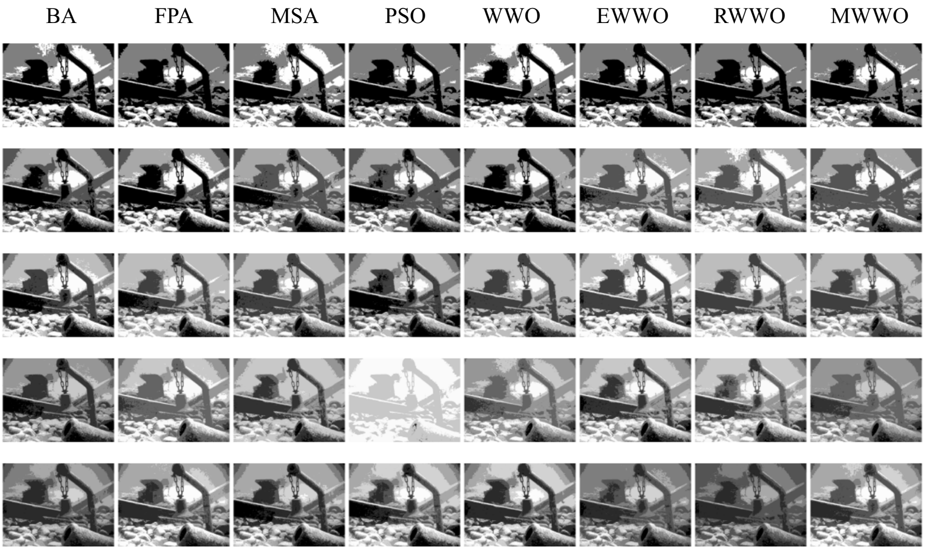

Fig. 6 Segmented images of Test 2

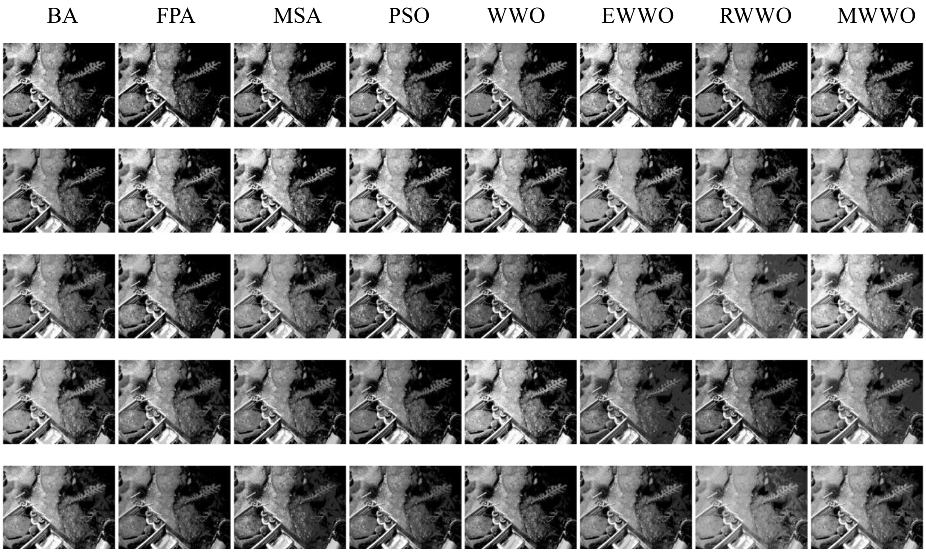

Fig. 7 Segmented images of Test 3

information the algorithm contains. Compared with other algorithms, MWWO not only obtains better SSIMs, but also contains more segmentation information. In other words, the segmented images obtained by MWWO are relatively close to the original images. Each algorithm has a total of 50 SSIMs, and 36 SSIMs of the MWWO are the best in all algorithms. The experimental results show that MWWO has higher similarity, higher calculation accuracy and a better segmentation ability.

The p value of the Wilcoxon rank-sum test [49] is used to evaluate the significance of the difference between MWWO and other algorithms. Table 9 gives the p value of the Wilcoxon rank-sum test. $p < 0.05$ indicates a significant difference between

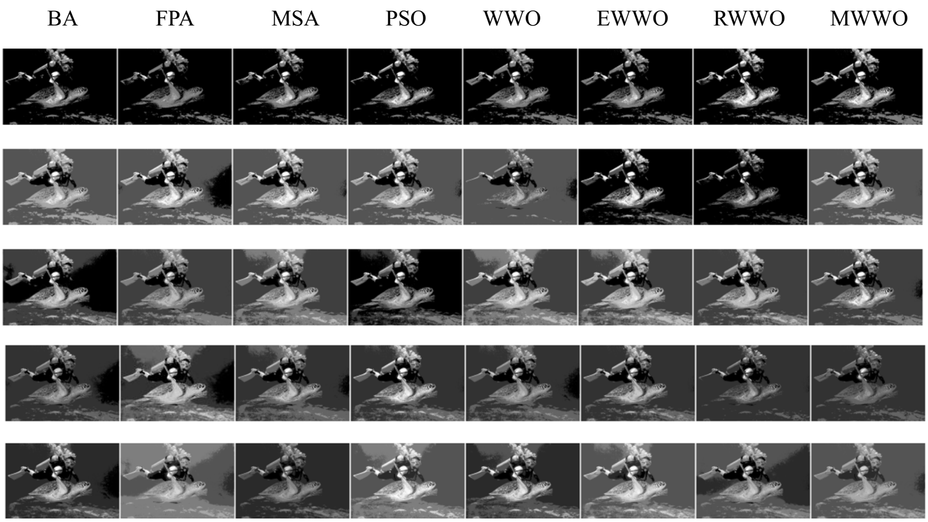

Fig. 8 Segmented images of Test 4

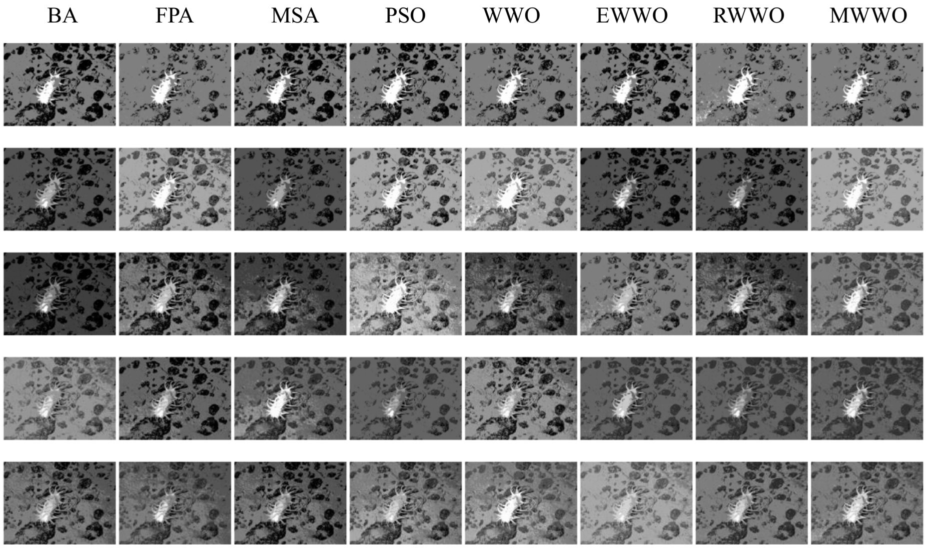

Fig. 9 Segmented images of Test 5

MWWO and the other algorithms. $p > 0.05$ indicates no significant difference between MWWO and the other algorithms. The experimental results show that there is a significant difference between MWWO and other algorithms and the data are not obtained by accident.

Figures 5, 6, 7, 8, 9, 10, 11, 12, 13 and 14 give the segmented images of each algorithm under different threshold levels. The segmentation effect of underwater images is better as the threshold level increases. The segmented images contain more valuable

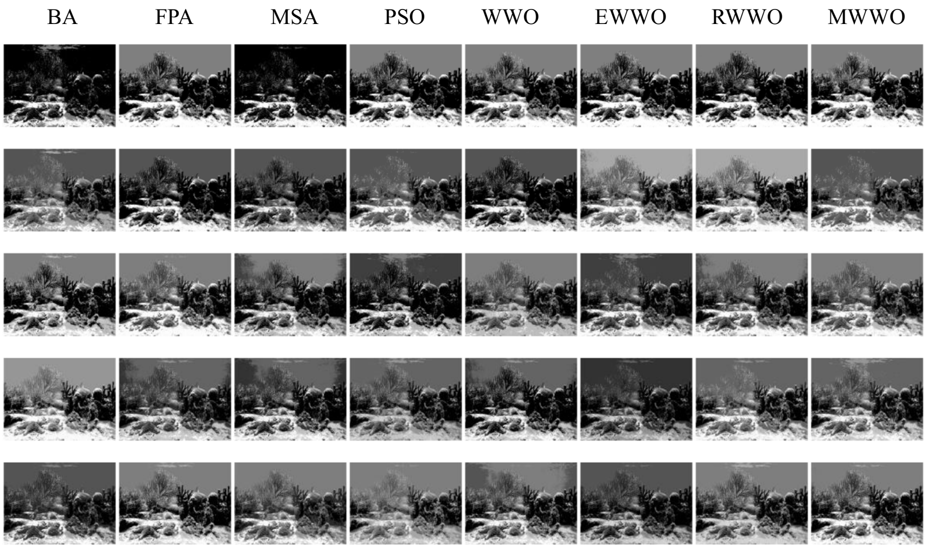

Fig. 10 Segmented images of Test 6

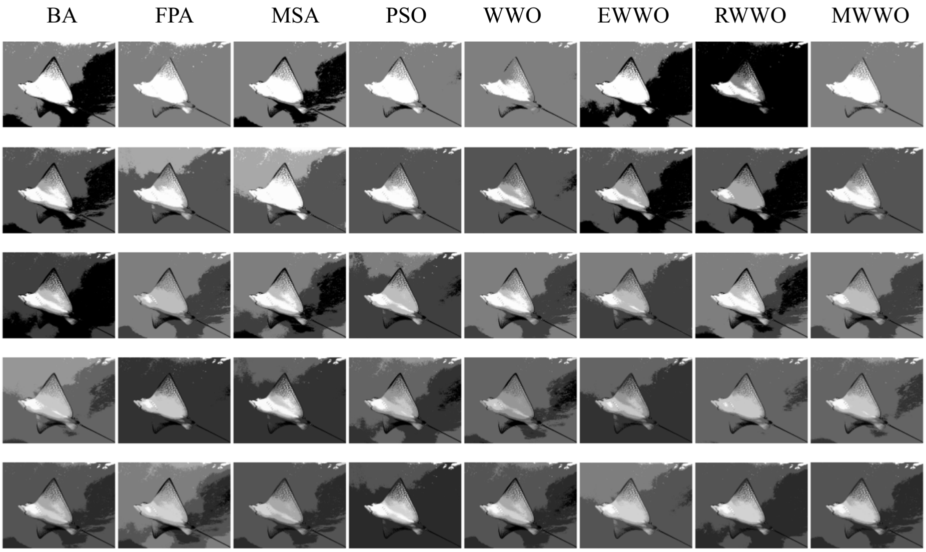

Fig. 11 Segmented images of Test 7

information. MWWO based on Kapur's entropy method is used to solve underwater multilevel thresholding image segmentation. Compared with other algorithms, MWWO has stronger robustness and better segmentation performance to obtain better segmented images. The segmentation effect of MWWO is closer to the original image. MWWO obtains the optimal fitness values and the best threshold values, which shows that MWWO can avoid falling into the local optimum and enhance the global search ability to obtain the optimal solution. In addition, MWWO has higher calculation accuracy and stronger search performance. The population size of all algorithms is 30,

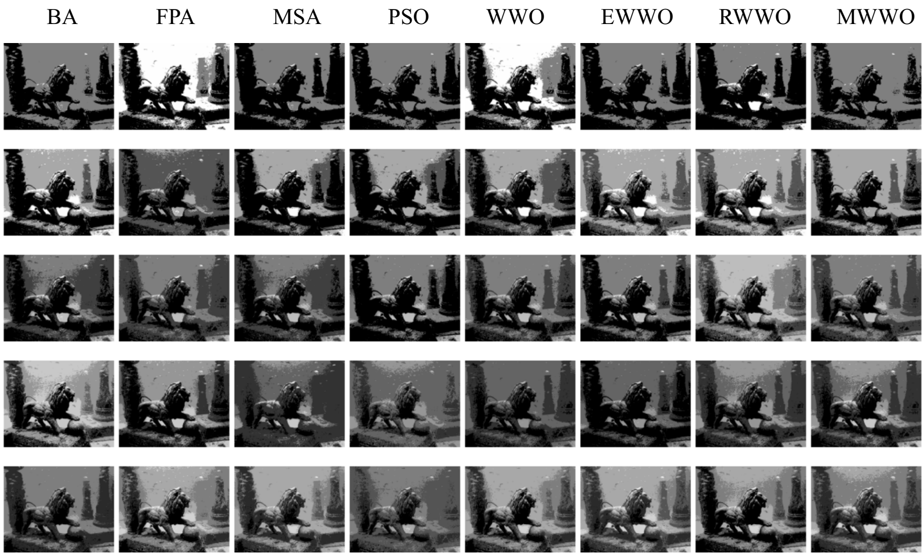

Fig. 12 Segmented images of Test 8

Fig. 13 Segmented images of Test 9

the maximum number of iterations is 100, and the number of independent runs is 30. MWWO has the elite opposition-based learning strategy and the ranking-based mutation operator added. The calculation accuracy of MWWO has been greatly improved, but MWWO consumes more time compared to the basic WWO, EWWO and RWWO. The PSNRs and SSIMs of MWWO are obviously superior to those of other algorithms, which shows that MWWO has low distortion and higher structure similarity. The Wilcoxon's rank-sum test is used to verify whether there is a significant difference between MWWO and other algorithms. In summary, MWWO has higher calculation accuracy, stronger robustness and better segmentation performance such that it can effectively solve the underwater image segmentation problem.

Statistically, MWWO is based on shallow water wave theory, which simulates propagation, refraction and breaking for global optimization. MWWO can solve the underwater image segmentation problem for the following reasons. First, MWWO has the characteristics of a simple algorithm framework, fewer control parameters and a smaller population size. Second, the elite opposition-based learning strategy increases the diversity of the population and avoids falling into the local optimum, and the ranking-based mutation operator improves the selection probability. Two strategies can achieve complementary advantages to improve the calculation accuracy of the basic WWO. Third, MWWO can avoid premature convergence and expand the search space. Meanwhile, the MWWO can effectively balance exploration and exploitation to obtain the global optimal solution. To summarize, MWWO is an effective and feasible method for solving the underwater image segmentation problem.

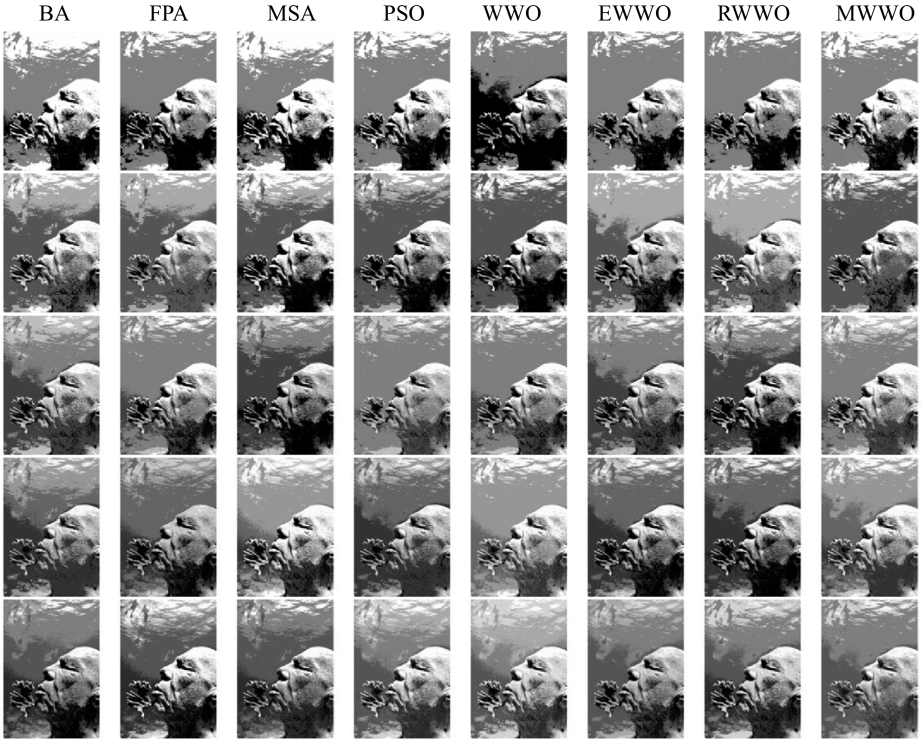

Fig. 14 Segmented images of Test 10

7 Conclusions and future research

In this paper, the elite opposition-based learning strategy and the ranking-based mutation operator are added into the basic WWO to improve its calculation accuracy. MWWO is proposed, which is used to solve the underwater image segmentation problem. The purpose of image segmentation is to obtain the optimal threshold values by maximizing the fitness value of Kapur's entropy method. The larger the threshold level is, the better the segmentation effect for an underwater image. MWWO has a strong global search ability to find the optimal solution. Compared with other algorithms, the MWWO can obtain segmented images with more information and have higher segmentation accuracy. As the threshold level increases, MWWO can balance the global search ability and the local search ability to obtain better segmented images. The experimental results indicate that MWWO has higher calculation accuracy and a better segmentation effect according to the fitness value, the threshold values, the execution time, the PSNR, the SSIM and the Wilcoxon's rank-sum test. Meanwhile, MWWO has stronger robustness and practicability to successfully solve the task of underwater image segmentation.

In future research, MWWO will be used to solve complex underwater image segmentation and high threshold color image segmentation. Meanwhile, various thresholding techniques will be applied to obtain the optimal threshold values and compare the accuracy and complexity, such as Tsallis entropy, Renyi entropy, cross entropy, fuzzy entropy, and Otsu's method. This work will further verify the segmentation performance of MWWO. In addition, the basic WWO will be added to an effective strategy or combined with other optimization algorithms to improve the convergence speed and calculation accuracy. The proposed algorithm will be used to solve more complex optimization problems.

Acknowledgments This work was partially funded by the National Nature Science Foundation of China under Grant No. 51679057, and partly supported by the Province Science Fund for Distinguished Young Scholars under Grant No. J2016JQ0052.

References

1. Abualigah LM (2020) Multi-verse optimizer algorithm: a comprehensive survey of its results, variants, and applications. Neur Comput Appl 1–21
2. Abualigah LM, Diabat A (2020) A novel hybrid antlion optimization algorithm for multi-objective task scheduling problems in cloud computing environments. Clust Comput 1–19
3. Abualigah LM, Khader AT (2017) Unsupervised text feature selection technique based on hybrid particle swarm optimization algorithm with genetic operators for the text clustering. J Supercomput 73(11):4773–4795
4. Abualigah LM, Khader AT, Hanandeh ES (2017) A new feature selection method to improve the document clustering using particle swarm optimization algorithm. J Comput Sci 25:456–466
5. Abualigah LM, Khader AT, Hanandeh ES (2018) A combination of objective functions and hybrid krill herd algorithm for text document clustering analysis. Eng Appl Artif Intell 73:111–125
6. Abualigah LM, Khader AT, Hanandeh ES (2018) Hybrid clustering analysis using improved krill herd algorithm. Appl Intell 48:4047–4071
7. Akay B (2013) A study on particle swarm optimization and artificial bee colony algorithms for multilevel thresholding. Appl Soft Comput 13(6):3066–3091
8. Aldahdooh A, Masala E, Van Wallendael G, Barkowsky M (2018) Framework for reproducible objective video quality research with case study on PSNR implementations. Digit Signal Prog 77:195–206
9. Ayala HVH, dos Santos FM, Mariani VC, dos Santos CL (2015) Image thresholding segmentation based on a novel beta differential evolution approach. Expert Syst Appl 42(4):2136–2142
10. Bao X, Jia H, Lang C (2019) A novel hybrid Harris hawks optimization for color image multilevel Thresholding segmentation. IEEE Access 7:76529–76546
11. Bhandari AK, Singh VK, Kumar A, Singh GK (2014) Cuckoo search algorithm and wind driven optimization based study of satellite image segmentation for multilevel thresholding using Kapur's entropy. Expert Syst Appl 41(7):3538–3560
12. Bohat VK, Arya KV (2019) A new heuristic for multilevel thresholding of images. Expert Syst Appl 117: 176–203
13. Breve F (2019) Interactive image segmentation using label propagation through complex network. Expert Syst Appl 123:18–33
14. Chen W, Yue H, Wang J, Wu X (2014) An improved edge detection algorithm for depth map inpainting. Opt Lasers Eng 55:69–77
15. Díaz-Cortés MA, Ortega-Sánchez N, Hinojosa S, Oliva D, Cuevas E, Rojas R, Demin A (2018) A multi-level thresholding method for breast thermograms analysis using dragonfly algorithm. Infrared Phys Technol 93:346–361
16. Elaziz MA, Ewees AA, Hassanien AE (2017) Whale optimization algorithm and moth-flame optimization for multilevel thresholding image segmentation. Expert Syst Appl 83:242–256
17. Elaziz MA, Oliva D, Ewees AA, Xiong S (2019) Multi-level thresholding-based grey scale image segmentation using multi-objective multi-verse optimizer. Expert Syst Appl 125:112–129
18. Emberton S, Chittka L, Cavallaro A (2018) Underwater image and video dehazing with pure haze region segmentation. Comput Vis Image Underst 168:145–156
19. Fu KS, Mui JK (1981) A survey on image segmentation. Pattern Recogn 13(1):3–16
20. Galdran A, Pardo D, Picón A, Alvarez-Gila A (2015) Automatic red-channel underwater image restoration. J Vis Commun Image Represent 26:132–145
21. Gao H, Fu Z, Pun CM, Hu H, Lan R (2018) A multi-level thresholding image segmentation based on an improved artificial bee colony algorithm. Comput Electr Eng 70:931–938

22. Gong W, Cai Z (2013) Differential evolution with ranking-based mutation operators. IEEE T Cybern 43(6): 2066–2081
23. He L, Huang S (2017) Modified firefly algorithm based multilevel thresholding for color image segmentation. Neurocomputing 240:152–174
24. Hinojosa S, Dhal KG, Elaziz MA, Oliva D, Cuevas E (2018) Entropy-based imagery segmentation for breast histology using the stochastic fractal search. Neurocomputing 321:201–215
25. Hou G, Pan Z, Wang G, Yang H, Duan J (2019) An efficient nonlocal variational method with application to underwater image restoration. Neurocomputing 369:106–121
26. Jia H, Ma J, Song W (2019) Multilevel Thresholding segmentation for color image using modified moth-flame optimization. IEEE Access 7:44097–44134
27. Kannan SS, Ramaraj N (2010) A novel hybrid feature selection via symmetrical uncertainty ranking based local memetic search algorithm. Knowledge-Based Syst 23(6):580–585
28. Kapur JN, Sahoo PK, Wong AKC (1985) A new method for gray-level picture thresholding using the entropy of the histogram. Comp Vis Graph Image Process 29(3):273–285
29. Kennedy J, Eberhart RC (2002) Particle swarm optimization. Int Conf Netw 4:1942–1948
30. Lee SH, Koo HI, Cho NI (2010) Image segmentation algorithms based on the machine learning of features. Pattern Recogn Lett 31(14):2325–2336
31. Li X, Song J, Zhang F, Ouyang X, Khan SU (2016) MapReduce-based fast fuzzy c-means algorithm for large-scale underwater image segmentation. Futur Gener Comput Syst 65:90–101
32. Li Y, Bai X, Jiao L, Xue Y (2017) Partitioned-cooperative quantum-behaved particle swarm optimization based on multilevel thresholding applied to medical image segmentation. Appl Soft Comput 56:345–356
33. Liu X, Zhang XY (2020) NOMA-based resource allocation for cluster-based cognitive industrial internet of things. IEEE Trans Ind Inform 16(8):5379–5388
34. Liu X, Jia M, Zhang X, Lu W (2019) A novel multichannel internet of things based on dynamic Spectrum sharing in 5G communication. IEEE Internet Things J 6(4):5962–5970
35. Lu Z, Qiu Y, Zhan T (2019) Neutrosophic C-means clustering with local information and noise distance-based kernel metric image segmentation. J Vis Commun Image Represent 58:269–276
36. Mirjalili S, Lewis A (2016) The whale optimization algorithm. Adv Eng Softw 95:51–67
37. Mohamed AA, Mohamed YS, Elgaafary AA, Hemeida AM (2017) Optimal power flow using moth swarm algorithm. Electr Power Syst Res 142:190–206
38. Ouadfel S, Taleb-Ahmed A (2016) Social spiders optimization and flower pollination algorithm for multilevel image thresholding: a performance study. Expert Syst Appl 55:566–584
39. Pare S, Kumar A, Bajaj V, Singh GK (2017) An efficient method for multilevel color image thresholding using cuckoo search algorithm based on minimum cross entropy. Appl Soft Comput 61:570–592
40. Pare S, Bhandari AK, Kumar A, Singh GK (2018) A new technique for multilevel color image thresholding based on modified fuzzy entropy and Lévy flight firefly algorithm. Comput Electr Eng 70:476–495
41. Sambandam RK, Jayaraman S (2018) Self-adaptive dragonfly based optimal thresholding for multilevel segmentation of digital images. J King Saud Univ-Comp Info Sci 30(4):449–461
42. Satapathy SC, Raja NSM, Rajinikanth V, Ashour AS, Dey N (2018) Multi-level image thresholding using Otsu and chaotic bat algorithm. Neural Comput & Applic 29(12):1285–1307
43. Shen L, Fan C, Huang X (2018) Multi-level image thresholding using modified flower pollination algorithm. IEEE Access 6:30508–30519
44. Sun G, Zhang A, Yao Y, Wang Z (2016) A novel hybrid algorithm of gravitational search algorithm with genetic algorithm for multi-level thresholding. Appl Soft Comput 46:703–730
45. Tang N, Zhou F, Gu Z, Zheng H, Yu Z, Zheng B (2018) Unsupervised pixel-wise classification for Chaetoceros image segmentation. Neurocomputing 318:261–270
46. Van DHMP, De Lange SC, Zalesky A, Zalesky A, Seguin C, Yeo BT (2017) Proportional thresholding in resting-state fMRI functional connectivity networks and consequences for patient-control connectome studies: issues and recommendations. Neuroimage 152:437–449
47. Vasamsetti S, Mittal N, Neelapu BC, Sardana HK (2017) Wavelet based perspective on variational enhancement technique for underwater imagery. Ocean Eng 141:88–100
48. Wang Z, Bovik AC, Sheikh HR, Simoncelli EP (2004) Image quality assessment: from error visibility to structural similarity. IEEE Trans Image Process 13(4):600–612
49. Wilcoxon F (1945) Individual comparisons by ranking methods. Biom Bull 1(6):80–83
50. Yang X (2012) Flower pollination algorithm for global optimization. International Conference on Unconventional Computation, pp 240-249
51. Yang XS, He XS (2013) Bat algorithm: literature review and applications. Int J Bio-Inspired Comput 5(3): 141–149

52. Zheng YJ (2015) Water wave optimization: a new nature-inspired metaheuristic. Comput Oper Res 55:1–11
53. Zhou Y, Wang R, Luo Q (2016) Elite opposition-based flower pollination algorithm. Neurocomputing 188(188):294–310
54. Zhou Y, Yang X, Ling Y, Zhang J (2018) Meta-heuristic moth swarm algorithm for multilevel thresholding image segmentation. Multimed Tools Appl 77(18):23699–23727